

AFML-TR-65-231

ADO 620734

OFFICIAL FILE COPY

THE RELATIONSHIPS BETWEEN POLYMERS AND GLASS TRANSITION TEMPERATURES

O. G. Lewis
L. V. Gallacher
American Cyanamid Company

TECHNICAL REPORT AFML-TR-65-231

JULY 1965

AIR FORCE MATERIALS LABORATORY
RESEARCH AND TECHNOLOGY DIVISION
AIR FORCE SYSTEMS COMMAND
WRIGHT-PATTERSON AIR FORCE BASE, OHIO

BEST AVAILABLE COPY

20040303382

NOTICES

When Government drawings, specifications, or other data are used for any purpose other than in connection with a definitely related Government procurement operation, the United States Government thereby incurs no responsibility nor any obligation whatsoever; and the fact that the Government may have formulated, furnished, or in any way supplied the said drawings, specifications, or other data, is not to be regarded by implication or otherwise as in any manner licensing the holder or any other person or corporation, or conveying any rights or permission to manufacture, use, or sell any patented invention that may in any way be related thereto.

Qualified requesters may obtain copies of this report from the Defense Documentation Center (DDC), Cameron Station, 5010 Duke Street, Alexandria, Virginia 22314.

This report has been released to the Clearing House for Federal Scientific and Technical Information, Washington 25, D. C., for sale to the general public.

Copies of this report should not be returned to the Research and Technology Division unless return is required by security considerations, contractual obligations, or notice on a specific document.

THE RELATIONSHIPS BETWEEN POLYMERS AND

GLASS TRANSITION TEMPERATURES

O. G. Lewis
L. V. Gallacher
American Cyanamid Company

Technical Report AFML-TR-65-231
July 1965

BEST AVAILABLE COPY

FOREWORD

This report was prepared by the Central Research Division of American Cyanamid Company, Stamford, Connecticut, under USAF Contract No. AF 33(657)-11224. The contract was initiated under Project No. 7342, "Fundamental Research on Macromolecular Materials and Lubrication Phenomena," Task No. 734203, "Fundamental Principles Determining the Behavior of Macromolecules." It was administered under the direction of The Air Force Materials Laboratory, Research and Technology Division, with Dr. Ivan Goldfarb as project engineer.

This report covers work conducted from June 1963 to May 1965. The authors are indebted to Prof. J. H. Gibbs for helpful discussions. The assistance of Dr. Maurice King in the mathematical analysis is gratefully acknowledged.

The manuscript was released by the authors 8 June 1965 for publication as an R & D Technical Report.

This technical report has been reviewed and is approved.



WILLIAM E. GIBBS
Chief, Polymer Branch
Nonmetallic Materials Division
Air Force Materials Laboratory

ABSTRACT

A study of some empirical and theoretical functions for the effect of temperature on liquid viscosity indicated that the viscosities of the *n*-alkanes are well represented by the equation $\log (\eta/d) = \log (A/\bar{T}) + B/(T-T_0)$, where *d* is the density and *A*, *B* and *T*₀ are smooth functions of chain length. The effect of increasing static pressure is to increase *A* and *T*₀, while *B* is only slightly affected. A relaxation theory developed by J. H. Gibbs relates *B* to the barrier to rotation about chain bonds. The *T*₀ (*n*) values are predicted for *n*-alkanes of more than *n*=6 carbon atoms by the Gibbs-DiMarzio theory with a flex energy of 490.8 cal./mole, in agreement with estimates by other methods. A diagrammatic method for evaluating steric effects in polymer chains was developed, based on the Pitzer model for alkanes. Some excluded volume effects in rings and short chains of the -CX₂- type are elucidated in this way. An empirical approach to estimation of flex energy and hence *T*₀ is suggested. A statistical-mechanical theory of the glass transition was developed, based on the concept that the observable communal entropy is time dependent. At *T*_g a contribution to the communal entropy due to backbone motions disappears, giving rise to a time-dependent glass temperature. Glass temperatures are theoretically predicted with good accuracy from viscosity data obtained far above *T*_g. The Eyring transition state theory for relaxation processes was modified to conform with observed polymer behavior. The activation free energy, enthalpy and entropy at the glass temperature were evaluated for several polymers. Intermolecular interactions in liquid alkanes were studied, and an additive property $Q = (B_p V)^{0.7240}$ was found, where *B_p* is the Antoine vapor pressure constant, and *V* the molar volume. *Q* is dependent on the number of C atoms, the number of side branches, and the number of pairs of vicinal branches.

TABLE OF CONTENTS

	PAGE
1. Mechanism of Relaxation in Polymers	1
2. Pressure Coefficient of the Glass Temperature	12
3. Test of the Gibbs-DiMarzio Theory	24
4. Estimation of Flex Energy	29
5. The Cell Model of the Glass Transition	37
6. Transition State Thermodynamics in the Glass Transition Region	48
7. Intermolecular Interactions	61

TABLES

	PAGE
I. Estimated Variance from Viscosity-Temperature Functions	5
II. Estimates of Parameters in Equation (1) for <u>n</u> -Alkanes	6
III. Estimates of Parameters in Equation (3) for <u>n</u> -Alkanes	7
IV. Estimates of Parameters in Equation (13) for <u>n</u> -Alkanes	8
V. Estimates of Parameters in Equation (17) for <u>n</u> -Alkanes	9
VI. Effect of Temperature on Shift Factors	15
VII. Effect of Pressure on Viscosity of 9-(2-Cyclohexylethyl)heptadecane	18
VIII. Effect of Pressure on Viscosity of 9-(2-Phenylethyl)heptadecane	19
IX. Effect of Pressure on Viscosity of Perhydrochrysene	20
X. Effect of Pressure on Viscosity of Dodecahydrochrysene	21
XI. Gibbs-DiMarzio Equation Using Data from Heptane to Eicosane	27
XII. Electrostatic and Steric Interaction Energies in PVC	33
XIII. Comparison of Flex Energies ϵ by Different Methods	35
XIV. Glass Temperatures of Polystyrene Calculated with Equation (34)	41
XV. T_g Values Computed Using Equations (12) and (31)	43
XVI. T_g Values Computed for <u>n</u> -Alkanes Using Equation (39)	45
XVII. Activation Energies for <u>n</u> -Alkanes	49

	PAGE
XVIII. Transition State Parameters at T_g for Dielectric Relaxation, Based on Saito's Data	53
XIX. Transition State Parameters at T_g for Viscous Flow	54
XX. Transition State Parameters at T_g Based on Eyring Viscosity Theory	56
XXI. Constants for the n -Paraffin Hydrocarbons	62
XXII. $B_p = \left[\frac{d}{m} (a_1 n + b_1)^2 + 592.48 \right] \left[\frac{(298.15 - T_o)^2}{406,750} \right]$	63
XXIII. $B_p = \frac{d}{m} [a_2 n + b_2]^{c2}$	64
XXIV. $B_p = d[a_3 n + b_3]^{c3}$	66
XXV. $T_o = B_p[a_4 n + b_4]^{c4}$	67
XXVI. $T_o = \frac{d}{m} [a_5 n + b_5]^{c5}$	68
XXVII. $T_o = d[a_6 n + b_6]^{c6}$	69
XXVIII. Correlations for Intermolecular Interactions	70
XXIX. Effect of Vicinal Side Groups on Q	71

1. Mechanism of Relaxation in Polymers

The temperature dependence of the viscosities of even simple liquids such as the *n*-alkanes cannot be adequately represented by the Arrhenius equation, since it is generally found that the activation energy for flow increases as the temperature is reduced. This effect is more pronounced in high polymers, and is most spectacular in the transition zone just above the glass temperature. Miller¹ has pointed out that the empirical equation proposed independently by Fulcher² and by Tamman and Hesse³,

$$\log \eta = \log A + B/(T-T_0), \quad (1)$$

is of particular interest not only because of the precision with which it fits accurate viscosity data on most liquids over a wide temperature range, but also because it can be transformed into the WLF⁴ equation,

$$\log a_T = -C_1(T-T_s)/(C_2 + T-T_s), \quad (2)$$

which is widely used to represent the temperature dependence of relaxation processes in polymers. In these equations, η is the shear viscosity, $a_T = \eta/\eta_s$, η_s is the viscosity at a reference temperature T_s , and A , B , T_0 , C_1 and C_2 are adjustable parameters. It can be shown that $C_2 = T_s - T_0$ and $C_1 C_2 = B$.

Equation (1) indicates that $\eta \rightarrow \infty$ at a temperature T_0 not necessarily equal to zero. The statistical-mechanical theory of glass formation developed by Gibbs and DiMarzio⁵ predicts just this type of behavior. It is therefore not unreasonable to identify T_0 with the point at which the configurational entropy of the liquid goes to zero. This is estimated⁶ to be 40 to 50° below the glass temperature, and can be calculated by the relationships given by Gibbs and DiMarzio, if the "flex energy" (see Section 3) in their theory is known. The purpose of this portion of the program was to determine T_0 for chains for which the flex energy is known from independent measurements, for comparison with the theoretical prediction.

The compilation of selected values of the properties of hydrocarbons published by the American Petroleum Institute's Research Project 44⁷ is considered the most reliable source of precise viscosities on n-alkanes over a wide temperature range. The complete set of data on each n-alkane from methane to eicosane was fitted to Equation (1) by machine computation using a non-linear least squares iteration procedure, to obtain the three adjustable parameters for each compound. Additional values were determined for n-alkanes of 28, 36 and 64 C atoms from data published by Doolittle⁸.

It was found empirically that Equation (3) gives a consistently

$$\log (\eta/d) = \log A + B/(T-T_0) \quad (3)$$

better fit to the data, as can be seen by comparison of the residual sum of squares for each compound in Table I. d is the liquid density. The use of kinematic instead of absolute viscosity is indicated by Eyring's⁹ treatment of viscous flow as a rate process and by the statistical theory of elasticity of chains¹⁰.

The precision of the estimates of all three parameters in equation (3) is rather poor, even though the viscosity predictions which they provide are quite good. This is because of the high correlations among the parameters, resulting perhaps from the fact that the measurements were made above the melting point, while T_0 is very much lower. Since the data were smoothed by the American Petroleum Institute workers before tabulating, no meaningful statistical statements can be made concerning the precision.

Gibbs and DiMarzio⁵ predicted that the (free energy) barrier restricting flow from one configurational state to another should increase with decreasing temperature as T_0 is approached from above, in agreement with the Fulcher equation, but this idea was expressed only qualitatively. Professor Gibbs has recently developed a quantitative relaxation theory, which he advanced during his last visit. Briefly, the theory is as follows:

A segment of polymer which is in some high energy configuration as a result of the application of a shear stress will relax to a configuration of lower energy at a rate

$$k_1 = A \exp (-zU/kT) \quad (4)$$

where z is the number of bonds in the segment and U is the average potential barrier. At least two configurations must be available in order for relaxation to occur, so in general, there will be some minimum configurational entropy required for relaxation. Denoting this by s^* , and observing that entropy is an extensive quantity,

$$s^* = S_c z^* / N \quad (5)$$

where S_c is the molar configuration entropy, z^* is the number of bonds in the segment of critical size for relaxation, and N is Avogadro's number. The average rate of relaxation for the entire system containing segments of all sizes is

$$k = \frac{\int_{z^*}^{\infty} A \exp(-2zU/kT) dz}{\int_{z^*}^{\infty} \exp(-zU/kT) dz} = \frac{A}{2} \exp\left(\frac{-z^*U}{kT}\right). \quad (6)$$

Hence, from Equation (5)

$$k = \frac{A}{2} \exp \frac{-Ns^*U}{kTS_c}. \quad (7)$$

Assuming that the configurational entropy is responsible for the increase in specific heat at T_g , we can write

$$S_c(T) = S_T - S_{T_0} = \int_{T_0}^T \Delta C_p d \ln T. \quad (8)$$

If it is assumed, as a first approximation, that ΔC_p is a constant, then

$$S_c(T) = \Delta C_p \ln (T/T_0). \quad (9)$$

Therefore,

$$k = \frac{A}{2} \exp \frac{-Ns^*U}{kT\Delta C_p \ln (T/T_0)} . \quad (10)$$

Setting the relaxation time τ equal to k^{-1} and combining the constants in (10) we have

$$\tau = A' \exp \frac{B'}{T \ln (T/T_0)} . \quad (11)$$

Professor Gibbs found that Equation (11) reproduced the WLF function over a wide range to within a few per cent. The Mathematical Analysis Group was requested to test the equation for goodness of fit to the *n*-alkane data. At the same time, an empirical modification of these equations was tested, in which a factor of T^{-1} is included in the pre-exponential term. The equations actually used, in addition to Equations (1) and (3), are listed below.

$$\log \eta = \log (A/T) + B/(T-T_0) \quad (12)$$

$$\log (\eta/d) = \log (A/T) + B/(T-T_0) \quad (13)$$

$$\log \eta = \log A + B/ T \ln (T/T_0) \quad (14)$$

$$\log (\eta/d) = \log A + B/ T \ln (T/T_0) \quad (15)$$

$$\log \eta = \log (A/T) + B/ T \ln (T/T_0) \quad (16)$$

$$\log (\eta/d) = \log (A/T) + B/ T \ln (T/T_0) \quad (17)$$

The sums of squares of the deviations from these functions, for the "best" choice of the adjustable parameters, three in every case, are shown in Table I. For 18 out of the 23 liquids, Equation (13) had the smallest deviation from the observed viscosities. The values of the parameters determined in this way are shown in Tables II through V

TABLE I

Estimated Variance* from Viscosity-Temperature Functions

Number of Carbon Atoms	Eq. (1)	Eq. (3)	Eq. (12)	Eq. (13)	Eq. (14)	Eq. (15)	Eq. (16)	Eq. (17)
1	0.1226	0.0042	0.0368	0.0713	0.1412	0.0035	0.0499	0.0597
2	2.950	1.951	1.441	0.387	3.116	2.337	1.789	0.5530
3	8.600	2.374	2.070	5.349	12.35	4.488	3.009	2.225
4	0.0737	0.1225	0.0686	0.1507	1.733	0.1976	-	0.1433
5	3.746	1.160	0.7940	0.2851	4.976	2.105	1.502	0.0580
6	2.188	0.6440	0.8253	0.0890	2.609	1.002	1.206	0.0803
7	3.845	1.196	1.226	0.0689	4.952	2.050	2.027	0.0889
8	1.632	0.5356	0.7397	0.0315	1.916	0.8053	1.026	0.0921
9	3.239	0.9733	1.334	0.0372	4.029	1.594	1.998	0.1438
10	2.567	0.7569	1.363	0.0646	2.965	1.118	1.800	0.1872
11	3.324	0.9800	1.740	0.0800	3.906	1.482	2.340	0.2493
12	3.263	0.9802	1.916	0.1307	3.696	1.405	2.436	0.3170
13	4.492	1.333	2.755	0.2259	5.060	1.888	3.443	0.4828
14	4.296	1.262	2.760	0.2393	4.749	1.753	3.371	0.4902
15	5.329	1.493	3.408	0.2564	5.922	2.108	4.185	0.5596
16	4.911	1.424	3.195	0.2719	5.395	1.976	3.885	0.5612
17	6.098	1.747	3.856	0.3024	6.818	2.485	4.777	0.6592
18	6.168	2.019	4.192	0.7660	6.734	2.646	4.994	1.076
19	8.424	2.629	5.766	0.9519	9.259	3.486	6.857	1.356
20	7.918	2.354	5.297	0.7366	8.744	3.195	6.384	1.134
28	2.422	1.094	1.785	0.5000	2.560	1.325	2.045	0.7050
36	1.850	0.7375	1.180	0.2250	2.120	1.000	1.490	0.4045
64	2.298	1.196	1.315	0.3950	2.900	1.715	1.850	0.7300

* $\sum_x (\log y - \log \hat{y})^2 \times 10^5 / (x-3)$, x = number of observations.

TABLE II

Estimates of Parameters in Equation (1) for n-Alkanes

<u>Number of Carbon Atoms</u>	<u>log A*</u>	<u>B (°K)</u>	<u>T₀ (°K)</u>
1	-1.533	45.31	37.0
2	-1.545	136.6	8.8
3	-1.409	157.0	21.3
4	-2.023	458.8	-68.7
5	-1.434	204.5	40.0
6	-1.537	263.4	36.3
7	-1.520	273.8	51.6
8	-1.634	345.4	41.2
9	-1.609	346.8	56.2
10	-1.698	412.6	46.2
11	-1.698	427.9	52.6
12	-1.749	477.3	46.2
13	-1.763	501.0	47.7
14	-1.800	542.3	42.9
15	-1.797	556.2	45.8
16	-1.818	588.8	41.9
17	-1.794	585.3	49.1
18	-1.818	619.4	43.9
19	-1.796	616.8	49.8
20	-1.798	631.4	50.3
28	-1.801	771.4	31.4
36	-1.605	708.2	64.3
64	-1.230	659.9	107.1

* For viscosity in cp.

TABLE III

Estimates of Parameters in Equation (3) for n-Alkanes

<u>Number of Carbon Atoms</u>	<u>log A*</u>	<u>B (°K)</u>	<u>T₀ (°K)</u>
1	-1.019	30.90	44.9
2	-1.076	90.70	25.8
3	-1.065	128.2	28.4
4	-1.374	261.8	-12.9
5	-1.073	154.7	54.5
6	-1.130	187.8	58.9
7	-1.132	202.6	71.3
8	-1.196	242.7	69.6
9	-1.191	252.1	81.2
10	-1.235	286.6	79.4
11	-1.236	300.1	85.4
12	-1.256	325.5	84.9
13	-1.259	339.9	88.1
14	-1.271	360.1	88.2
15	-1.265	369.3	91.8
16	-1.270	385.7	91.7
17	-1.254	387.9	96.9
18	-1.258	402.8	96.4
19	-1.238	402.2	101.6
20	-1.237	411.4	103.1
28	-1.249	524.8	86.1
36	-1.121	514.6	105.9
64	-0.829	522.9	133.7

* For viscosity in cs.

TABLE IV

Estimates of Parameters in Equation (13) for n-Alkanes

<u>Number of Carbon Atoms</u>	<u>ln A*</u>	<u>B (°K)</u>	<u>T₀ (°K)</u>
1	3.0615	18.132	62.652
2	3.5813	59.822	56.084
3	3.6442	142.73	44.995
4	3.6763	199.77	44.833
5	3.9639	152.57	33.711
6	4.0272	176.57	97.581
7	4.0425	215.33	104.91
8	4.0632	245.34	113.29
9	4.0726	273.69	119.40
10	4.0896	308.06	124.76
11	4.1094	334.79	129.27
12	4.1319	360.87	132.51
13	4.1549	383.41	135.76
14	4.1771	405.65	138.37
15	4.2100	420.65	142.00
16	4.2384	436.85	144.49
17	4.2773	446.53	148.30
18	4.3066	458.88	150.80
19	4.3520	462.59	154.99
20	4.3741	475.06	157.07
28	4.4808	628.37	146.66
36	4.7276	652.62	158.78
64	5.3347	734.61	174.92

* For viscosity in cs.

TABLE V

Estimates of Parameters in Equation (17) for n-Alkanes

<u>Number of Carbon Atoms</u>	<u>ln A*</u>	<u>B (°K)</u>	<u>T₀ (°K)</u>
1	3.1167	21.206	61.1
2	3.6812	89.775	49.1
3	3.8519	244.85	36.0
4	-	-	-
5	4.1277	231.49	73.0
6	4.1831	274.97	83.6
7	4.2263	328.52	91.0
8	4.2390	393.70	94.7
9	4.2718	435.67	101.8
10	4.2841	500.71	103.4
11	4.3154	541.18	107.5
12	4.3381	597.00	108.3
13	4.3673	635.47	110.7
14	4.3899	683.40	111.4
15	4.4265	705.97	114.8
16	4.4541	741.64	115.7
17	4.4978	747.92	120.0
18	4.5242	777.46	120.9
19	4.5720	771.80	126.0
20	4.5958	794.58	127.4
28	4.7228	1199.2	105.0
36	4.9945	1165.7	121.2
64	5.6579	1213.6	142.8

* For viscosity in cs.

for four of these functions. Except for Equation (1), all of these equations yield a set of T_0 values which increase smoothly with the number of carbon atoms. The estimates of T_0 for any one liquid vary somewhat from one equation to another, and there seems to be no way of choosing among them on grounds of physical reasonableness. Since we are primarily interested in the values of T_0 for long chains, an effort was made to locate viscosity data on higher polymers. Tung¹¹ reported zero shear melt viscosities as a function of temperature for branched and unbranched polyethylene fractions, which should be suitable for calculation of T_0 . However, the points were too scattered for a reliable estimate.

Aggarwal, et al.¹² reported viscosities at different temperatures for low density polyethylene fractions, and these were fitted to Equation (1). Two of the sets of data were too scattered to be useful, and T_0 for the other three ranged from <0 to $>220^\circ\text{K}$.

Marker, et al.¹³ gave melt viscosities for a whole polymer of low density polyethylene with $\bar{M}_n = 33,330$. The data fit Equation (1) with $T_0 = 33^\circ\text{K}$ and $B = 2,642^\circ\text{K}$. These values do not seem to fit in with the results for the *n*-paraffin series. It was concluded that the available viscosity data on polyethylene are not sufficiently accurate for our purposes, possibly due to shear degradation or oxidative degradation.

While this work was in progress, the paper by Karapet'yants and Yan¹⁴ appeared, giving the constants in Equation (1) for 35 hydrocarbons. However, these workers found it necessary to use a separate set of constants for the upper (>0.85 cps) and lower (<0.85) ranges of values, making a total of six adjustable parameters for each liquid. Furthermore, many of their T_0 values are negative, in contrast to those in Tables II through V all of which (except for butane) are positive. Other workers have also reported negative values of T_0 . This seems to result from the use of viscosity data at temperatures far above T_0 , and possibly from improper weighting of data.

The viscosity data of Fox and Flory¹⁵ on polystyrene fractions can be used to calculate $\log A$, B and T_0 as a function of degree of polymerization, P . The data had already been fitted to an equation of the same form as (1) by Williams¹⁶, and as Miller¹ has pointed out, the constants in Equation (1) can be obtained by a simple transformation. The resulting values of B and T_0 are shown plotted against P in Figure 1. Both B and T_0 approach limiting values above $P = 200$, and drop off rapidly below that. This type of behavior is predicted by the Gibbs-DiMarzio theory, but no attempt was made to fit the data to the theory, since Gibbs and DiMarzio had already obtained⁵ an excellent fit to the glass temperatures of these samples.

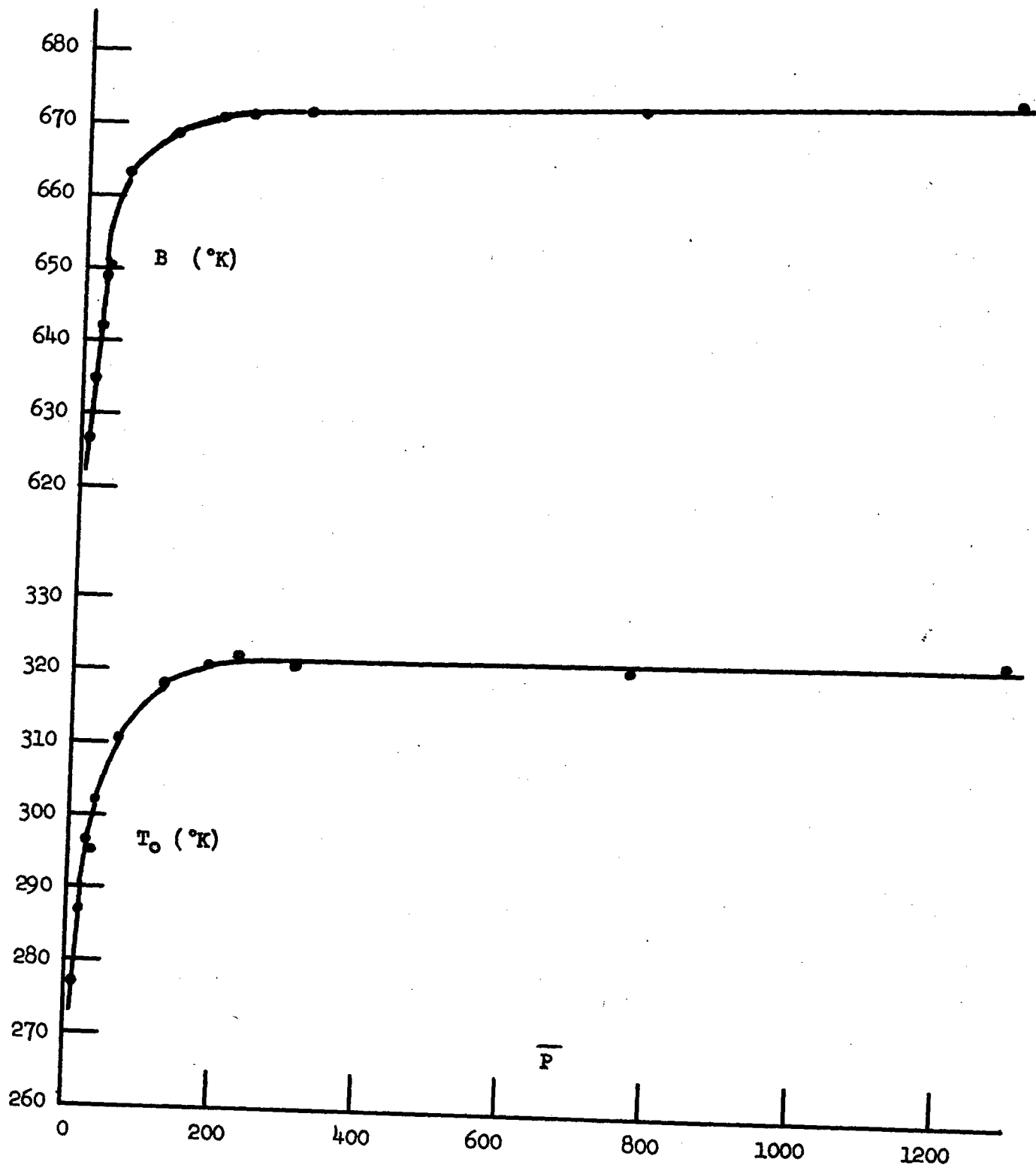


Figure 1

Constants in Equation (1) for Polystyrene

2. Pressure Coefficient of the Glass Temperature

When the temperature of a liquid is reduced, or its hydrostatic pressure increased, the liquid forms a glass (unless crystallization intervenes) at a characteristic temperature which increases with pressure. The location of this "glass temperature curve" on the phase diagram is one object of this study. Glass formation is preceded by a marked rise in viscosity, and this behavior is satisfactorily represented by Equation (13), for example.

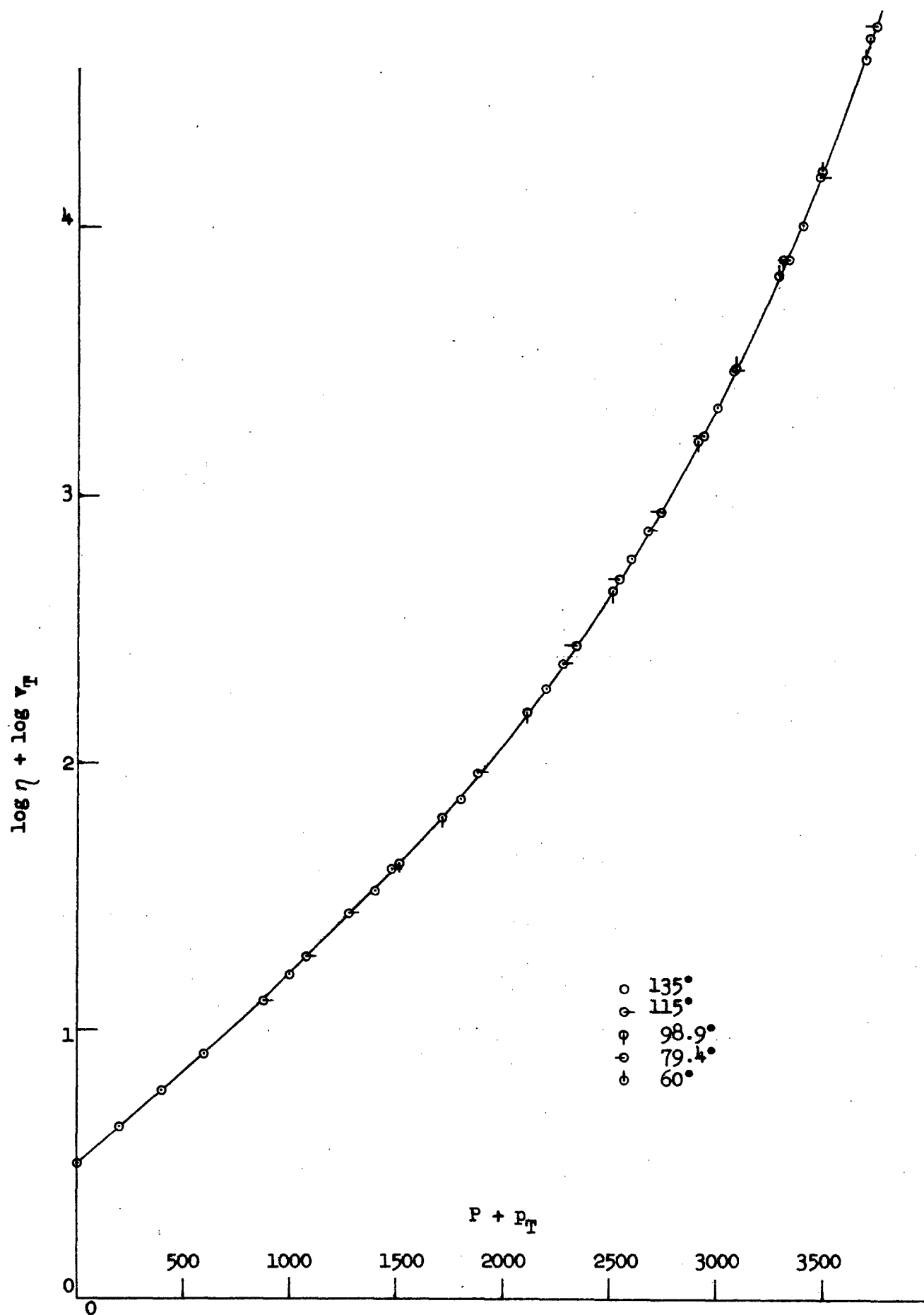
An attempt was made during this program to develop a theory for the effect of pressure on viscosity, to complete the picture phenomenologically. While successful to a degree, the adjustable parameters calculated from published data were complex functions of temperature, and furthermore, significant deviations from the predicted behavior were evident on plots of $\log \eta$ vs. pressure. On inspection of families of isotherms on these plots, it was noticed that the deviations show systematic trends with changing temperature. In fact, it was found that a suitable combination of vertical and horizontal shifts results in almost perfect superposition of all the isotherms. As an example, a master curve is shown in Figure 1 for 1, 2, 3, 4, 5, 6, 7, 8, 13, 14, 15, 16-dodecahydrochrysene, in which all the reported data¹⁷ for this liquid are superposed on the (extended) 135° isotherm. Two additional points obtained at 37.8° are not shown, since they would require compression of the viscosity scale to accommodate two more logarithmic decades, although they also superpose nicely.

The pressure scale for each isotherm was shifted horizontally by an amount p_T (atm.) and the viscosity scale was shifted vertically by an amount $\log v_T$ to produce the master curve in Figure 2. These shift factors were found to be well represented by the following functions of temperature:

$$p_T = 42.1 (135-t), \quad (18)$$

$$\log v_T = 3.175 (1000/T - 2.45), \quad (19)$$

where t is the temperature in degrees Centigrade and T is the absolute temperature. The coefficient of 42.1 atm. deg.⁻¹ in Equation (18) has the dimensions of a thermal pressure, and corresponds to a cohesive energy of 304 cal. cc.⁻¹ at 25°. The activation energy from Equation (19) is 14.5 kcal. mole⁻¹.



In order to determine T_0 as a function of pressure, it is necessary to extrapolate the master curve in Figure 2 to $\log v_T = \infty$. Designating the corresponding pressure on the master curve as $P^*(t)$, then the external pressure at T_0 is given by $P_0 = P^*(t) - p_T$, and the " T_0 , P_0 curve" for dodecahydrochrysene is predicted as

$$P_0 = P^*(135) - 42.1(135 - t). \quad (20)$$

The pressure coefficient of T_0 from Equation (20) is $1/42.1 = 0.0237$ deg. atm.⁻¹, which is at the upper end of the range (0.004 to 0.024) of values for ten substances tabulated by O'Reilly¹⁸ from direct observations of glass transitions.

Of the fourteen liquids studied by Lowitz, et al.¹⁷, sufficient data were reported on seven to give a critical test of the general validity of the temperature-pressure superposition principle. It was thought desirable to work with kinematic viscosities, η/d , since it had been found earlier that these obey the Fulcher equation more closely than absolute viscosities. The densities of some of the liquids were given in Reference 17, but had to be interpolated from values tabulated at different intervals in a previous publication¹⁹ for the others. The Mathematical Analysis Group was requested to perform the interpolations and to calculate $\log (\eta/d)$ and $\log \log (\eta/d)$. R. M. King provided the author with values of d , η/d , $\log (\eta/d)$ and $\log \log (\eta/d)$ at every temperature and pressure for which η was reported, for the seven liquids chosen.

It was found that the $\log (\eta/d)$ vs. P isotherms for perhydrochrysene could be accurately superposed by a suitable combination of vertical and horizontal shift factors, just as for dodecahydrochrysene. p_T was found to be linear in temperature, and $\log v_T$ was linear in T^{-1} . The activation energies and pressure coefficients for the two liquids are compared in Table VI, where it can be seen that the saturated compound has the lower activation energy and higher pressure coefficient, both indicative of a lower cohesive energy.

TABLE VI

Effect of Temperature on Shift Factors

	<u>Activation Energy</u> (kcal. mole ⁻¹)	<u>Pressure Coefficient</u> (deg. atm. ⁻¹)
Dodecahydrochrysene	14.5	0.0237
Perhydrochrysene	9.3	0.0263

The precision with which the viscosities of these two liquids fall on the master curve; the smooth trends in shift factors with changing temperature; and the physically reasonable values of the activation energies and pressure coefficients, all lend credence to the principle of temperature-pressure superposition. The situation is actually more complex than this, however, since the isotherms for the other five liquids studied do not superpose on a plot of $\log (\eta / d)$ vs. P . It was found that isotherms for these liquids could be superposed if plotted as $\log \log (\eta / d)$ vs. P , but it would be preferable to have a single form for the master curve, especially if a good analytical representation were known.

Since Equation (3) is known to fit the data at constant pressure over a wide temperature range on all the liquids for which it has been tested, it was decided to construct master isobars, which could then be fitted to Equation (3). A number of functions were tried before it was found that a simple plot of $\log \eta / d$ vs. temperature forms a family of isobars which exactly superpose when shifted by appropriate horizontal and vertical factors. The master curve is of the form

$$\log \eta / d - \log v_p = f(t - \theta_p) \quad (21)$$

The vertical shift factor v_p represents the effect of pressure on the parameter A in Equation (3), and the horizontal shift factor θ_p the effect on T_0 . The fact that the curves for all pressures superpose means that B is independent of pressure. B is equivalent to $C_1 C_2$ in the WLF equation, and it was originally proposed²⁰ that this is a universal constant with a value of 900° for all polymers.

Master curves of $\log \eta/d$ vs. t reduced to one atmosphere were constructed for perhydrochrysene, 9-(2-cyclohexylethyl)heptadecane and 9-(2-phenylethyl)heptadecane from the data of Lowitz, et al.¹⁷ The precision with which the points can be superposed is illustrated for perhydrochrysene in Figure 3. The shift factors $\log v_p$ and θ_p were found to be smoothly increasing functions of pressure, both slightly concave toward the pressure axis. Since

$$T_0(P) = T_0(1) + \theta_p, \quad (22)$$

the plot of θ_p against P represents a phase boundary for the glass-liquid transition.

The Ehrenfest condition for a second-order transition is

$$T_0^{-1} dT_0/dP = v \Delta\alpha / \Delta c_p, \quad (23)$$

where $\Delta\alpha$ is the difference in thermal coefficient of expansion below and above the transition point, and Δc_p the difference in specific heat. Since both thermal expansion and specific heat are reduced by compression, we might expect, from Equation (23) that $d \ln T_0/dP$ might be independent of pressure, at least over a limited range. However, it was found that the plots of $\log T_0$ vs. P were also concave toward the pressure axis.

The Mathematical Analysis Group was requested to determine the best least squares values of the parameters in Equation (3) under the restriction that B be independent of pressure, for the four liquids for which the most data are given in Reference 17. A computer program was written for the simultaneous estimation of the least squares values of B , $\log A$ and T_0 for the viscosities reported at eleven different pressures, a total of 23 parameters for each compound. At the same time, least-squares estimates were obtained for an unconstrained model in which B was permitted to vary with pressure, giving a total of 33 parameters for each compound. The parameters and the sums of squares of the deviations in $\log (\eta/d)$ for both models are given in Tables VII to X for the four liquids studied. The curve drawn in Figure 3 represents the values predicted from the least-squares parameters in Table IX with B constant. Figure 4 is a plot of P vs. T_0 for all four compounds.

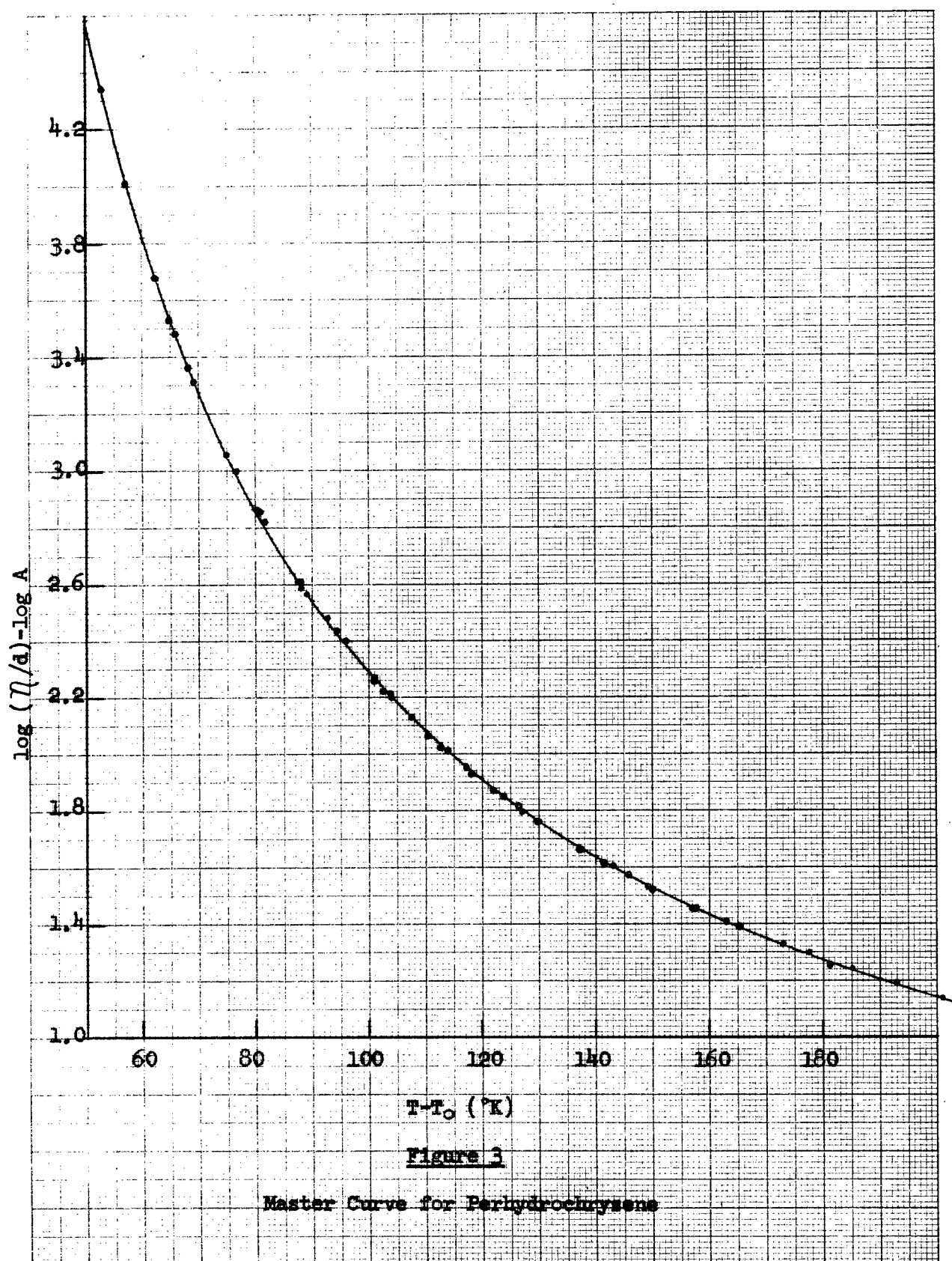


TABLE VII

Effect of Pressure on Viscosity of 9-(2-cyclohexylethyl)heptadecane

Pressure (atm.)	Number of Observations	Common Model		Individual Model		
		A	T ₀ (°K)	A	B (°K)	To(°K)
1	6	-1.4011	127.01	-1.0077	309.50	168.73
200	6	-1.3394	133.35	-0.89023	293.96	178.20
400	6	-1.2730	138.00	-0.82775	298.71	180.49
600	6	-1.2145	142.66	-0.82240	320.32	178.41
1000	6	-1.1074	150.74	-0.75037	337.61	180.71
1400	6	-1.0157	158.16	-0.80589	392.81	174.44
1800	6	-0.92987	164.53	-0.89000	455.92	167.41
2200	6	-0.84070	169.59	-0.98525	524.90	159.70
2600	6	-0.75391	174.18	-1.0408	578.04	155.59
3000	6	-0.66525	178.00	-1.0304	605.86	155.41
3400	6	-0.58103	181.66	-0.99841	622.91	156.99
RSS* x 10 ⁵		0566.74191				85.007407
B (°K)		470.75				

$$* \sum (\log y - \log \hat{y})^2 \times 10^5$$

TABLE VIII

Effect of Pressure on Viscosity of 9-(2-Phenylethyl)heptadecane

Pressure	Number of Observations	Common Model		Individual Model			
		A	T ₀ (°K)	A	B (°K)	T ₀ (°K)	RSS* x 10 ⁵
1	6	-1.1334	144.85	-1.0011	296.49	160.78	01.1815865
200	6	-1.0621	149.40	-0.81175	254.97	178.12	03.7633616
400	6	-1.0018	153.78	-0.73568	251.53	182.93	02.5830736
600	6	-0.95271	158.15	-0.72326	265.88	182.13	01.7287496
1000	6	-0.85701	165.39	-0.67208	283.69	183.22	01.7206529
1400	6	-0.77030	171.72	-0.61704	296.31	185.45	05.1074352
1800	6	-0.69190	177.52	-0.59689	317.05	185.45	09.5920434
2200	6	-0.61844	182.82	-0.60782	345.76	183.65	07.6963394
2600	6	-0.54585	187.25	-0.65148	384.79	179.43	04.6353024
3000	6	-0.47359	191.23	-0.69190	422.47	175.91	02.9991510
3400	6	-0.40733	195.15	-0.73653	459.14	173.25	03.1427884
RSS* x 10 ⁵		0261.54413	x 10 ⁵				44.150484
B (°K)		349.33					

$$*\sum(\log y - \log \hat{y})^2 \times 10^5$$

TABLE IX

Effect of Pressure on Viscosity of Parhydrochrysene

Pressure	Number of Observations	Common Model		Individual Model		
		A	To(°K)	A	B (°K)	To(°K)
1	6	-0.78028	206.95	-0.79156	232.41	206.00
200	6	-0.72160	215.22	-0.59391	196.13	224.67
400	6	-0.66363	222.91	-0.53040	196.79	231.53
600	6	-0.61192	230.60	-0.50216	204.05	236.82
1000	6	-0.50861	245.10	-0.45666	218.70	247.22
1400	6	-0.39617	258.25	-0.42681	234.55	257.37
1800	5	-0.29052	271.03	-0.40384	250.22	267.26
2200	4	-0.21236	284.47	-0.21505	229.66	284.37
2600	4	-0.090207	295.55	-0.21192	248.82	292.43
3000	3	0.019566	307.31	-1.0017	423.55	279.00
3400	2	0.10272	319.04	-	-	-
RSS* $\times 10^5$		0277.89735				53.3794236
B (°K)		299.17				

$$*\sum (\log y - \log \hat{y})^2 \times 10^5$$

TABLE X

Effect of Pressure on Viscosity of Dodecahydrochrysene

Pressure	Number of Observations	Common Model		Individual Model		
		A	To(°K)	A	B (°K)	To(°K)
1	5	-0.84187	248.43	-0.67989	181.40	257.78
200	5	-0.78964	256.91	-0.64502	187.48	263.95
400	5	-0.74298	264.88	-0.56400	183.54	272.16
600	5	-0.68528	271.78	-0.61819	205.16	274.09
1000	5	-0.55607	284.50	-0.62567	227.81	282.83
1400	4	-0.46228	297.92	-0.48710	220.90	297.29
1800	3	-0.36296	310.15	-0.74284	280.25	299.86
2200	3	-0.17706	319.68	-1.0739	355.97	301.29
2600	2	-0.10528	331.69	-	-	-
3000	-	-	-	-	-	-
3400	-	-	-	-	-	-
RSS* $\times 10^5$		0352.84006				58.69709968
B (°K)		217.08				

* $\sum (\log y - \log \hat{y})^2 \times 10^5$

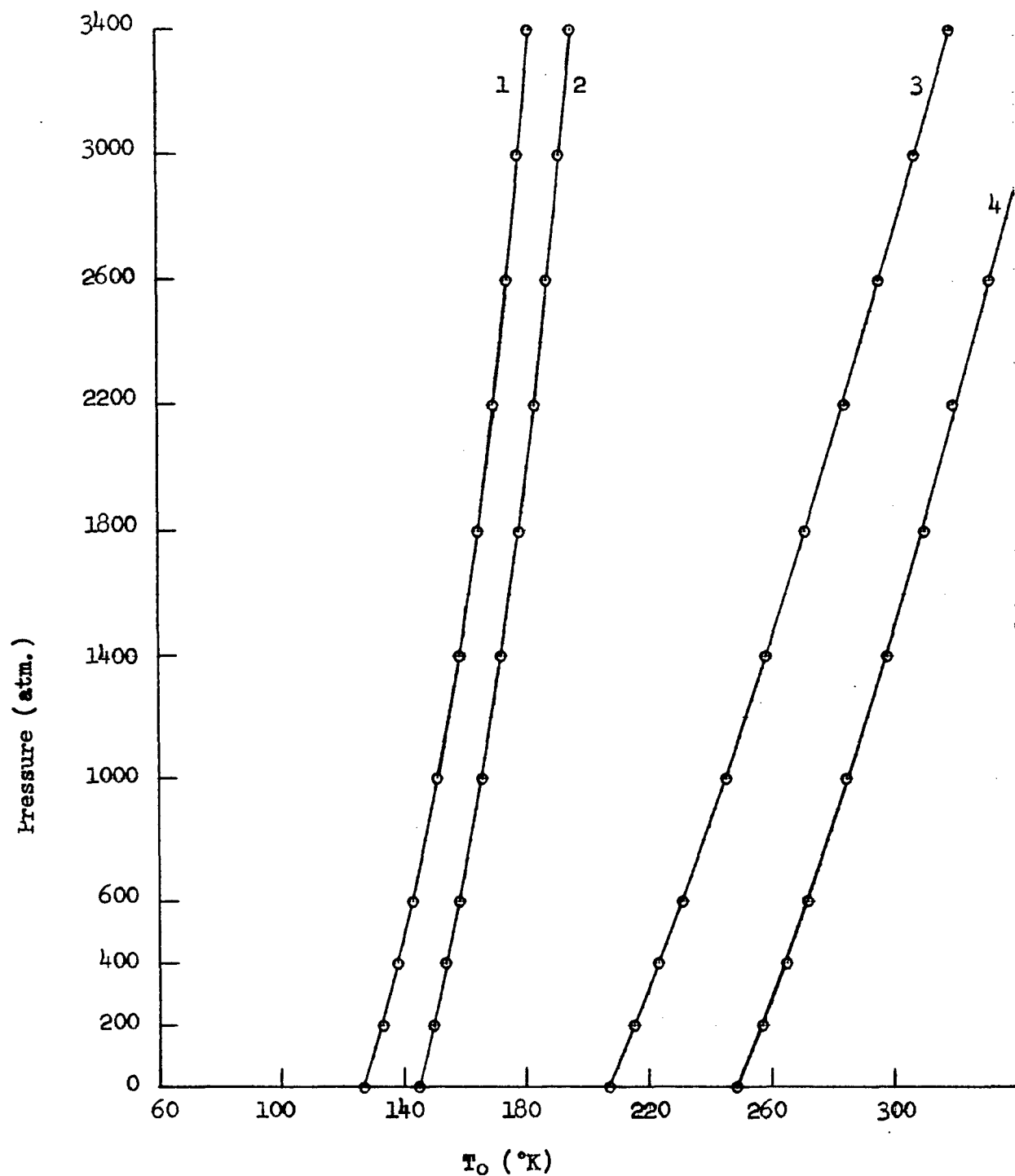


Figure 4

Effect of Pressure on T_0

1. 9-(2-Cyclohexylethyl)heptadecane
2. 9-(2-Phenylethyl)heptadecane
3. Perhydrochrysene
4. Dodecahydrochrysene

The residual sum of squares is lower for the 33 parameter unconstrained model, as expected. A statistical test of the variance ratios indicates that the difference is significant at the 99.5% confidence level, and hence that a single value of B, independent of pressure, is not supported by these data. However, it should be pointed out that the data were reported at integral pressures by interpolation of the raw data, so that the calculated variance does not give a true indication of error. To establish the validity of the model in which B is independent of pressure, a statistical test would have to be made on the original, unsmoothed data.

The fact that the parameter B in Equation (3) is only a slowly varying function of pressure, but different for each liquid, suggests that it is responsive primarily to intramolecular effects and much less to intermolecular interactions. According to Gibbs' relaxation theory (see Equation (10), Section I), $B = Ns^*U/k\Delta C_p$. Since N, s^* , k and ΔC_p are all constants, the small variation in B with pressure must be due to a small variation in U. It seems reasonable to identify U with the average intramolecular barrier to rotation about single chain bonds, which should be relatively insensitive to intermolecular separation.

3. Test of the Gibbs-DiMarzio Theory

The purpose of this section is to test the Gibbs-DiMarzio theory⁵ against the $T_0(n)$ values for the *n*-alkanes, obtained by applying Equation (3) to the reported viscosities, and to estimate the flex energy of a polymethylene chain by this means.

The Gibbs-DiMarzio theory considers a quasi-crystalline lattice model with vacant sites (free volume). Every bond of each chain is allowed $z'-1$ possible conformations, where z' is the valence of the chain atoms. One conformer is assumed to be of lower energy than the others, the average energy difference designated as ϵ .

The energy differences calculated⁵ from glass temperatures for several polymers have values which are reasonable for rotational energy levels, but have not been verified by independent means. The corresponding values of ϵ derived from dilute solution viscosity measurements and from thermoelastic measurements are for the most part questionable, as pointed out in recent compilations of published data^{21,22}. Only in the case of polyethylene do the results seem to be in complete accord with expectation, the energy difference by both solution and bulk measurements being about 500 cal./mole²³. Furthermore, this is the expected magnitude for a $-\text{CH}_2-$ chain from spectroscopic measurements on butane, pentane and hexane²⁴.

The Gibbs-DiMarzio theory was applied to values of T_0 calculated by fitting Equation (3) to viscosity-temperature data on the lower *n*-alkanes, to determine whether the trend with increasing chain length is correctly predicted with a flex energy ϵ of approximately 500 cal./mole.

The configurational entropy of a bulk polymer is calculated by the quasicrystalline lattice method developed by Huggins²⁵ and Flory²⁶ for the entropy of mixing polymer with a low-molecular-weight solvent. Solvent sites are left vacant in the case of bulk polymer, corresponding to a free volume fraction. The mixing is considered to take place in two stages: (1) disordering of the perfectly ordered polymer, and (2) mixing disordered polymer with solvent (vacancies). It is necessary to take account of the fact that there is an energy change in going from a state of perfect order to one of random arrangement. There is no way to estimate the magnitude of the change in intermolecular energy, so the energy change is attributed entirely to the intramolecular effect of rotations of single bonds into higher energy conformations. If the shape of the chain is sufficiently symmetrical when in its lowest energy level, then crystallization is predicted²⁷ to occur below a critical value of f , the fraction of bonds

rotated out of their ground states. If not, the number of configurations available to the system will continue to decrease as the temperature is reduced until it reaches such a low value that further changes occur at a negligible rate because of the energy barriers separating them. The system then remains frozen in one configuration at lower temperatures.

The relations given in Reference (5) yield the following expression for the entropy of disorder per atom when chains of n lattice-site-occupiers of valence z' are placed on a lattice of coordination number z :

$$\begin{aligned} \frac{S_c}{R} = & \frac{z-2}{2} \frac{\ln v}{1-v} + \frac{1}{2} \left(z-2 + \frac{zv}{1-v} \right) \ln \left[\frac{(z-2)n + 2}{znv} (1-v) + 1 \right] \\ & + n^{-1} \ln \frac{[(z-2)n + 2] (z-1)}{2} + \frac{n-3}{n} \left\{ \ln[1 + (z'-2) g] \right. \\ & \left. + \frac{(z'-2) g}{1 + (z'-2) g} \frac{\epsilon}{RT} \right\}. \end{aligned} \quad (24)$$

Here, v is the fraction of vacant lattice sites (free volume), $g = \exp(-\epsilon/RT)$ and ϵ is the difference between an average energy of "flexed" bonds and the energy of the preferred conformation.

Equation (24) has a number of interesting properties which should be pointed out. When $z=z'=4$ and S_c is set equal to zero to solve for ϵ/T_0 , negative values are obtained for $n=5$ or less, meaning that random packing is always possible no matter how stiff the chains, provided they are shorter than six units. Since we have T_0 data for chains of as few as five atoms, we assume that the lattice-site occupier is a single methylene group, and seek to reduce the entropy by varying some of the parameters in Equation (24). Adjustment of the free volume v over a reasonable range of values does little to improve the fit to the data. Hence it is expedient to neglect free volume in calculating the flex energy ϵ .

Gibbs and DiMarzio assumed that the conformational energy of each bond is independent of the conformations of neighboring bonds. In actuality, certain combinations of torsional angles result in large steric effects. In the case of polymethylene chain, in particular, a gauche bond followed immediately by a gauche rotation in the opposite direction (GG') is virtually excluded by reason of its high energy. Mathematical techniques for treating the problem of pairwise correlations of rotation have been developed by Lifson²⁸ and applied to the calculation of random coil dimensions by Nagai and Ishikawa²⁹ and by Hoeve³⁰, and to the entropy of melting by Starkweather and Boyd³¹. The decrease in entropy due to the exclusion of GG' pairs (pentane effect) is greatest when $\epsilon/T = 0$, and is negligible^{29,31} for $\epsilon/T \approx 5$ cal. deg.⁻¹ mole⁻¹. For $n \rightarrow \infty$, Equation (24) gives $\epsilon/T_0 = 3.81$ (for $v=0$ and $z=z'=4$), and ϵ/T_0 increases as n decreases. The formula given by Taylor³² for the fraction of "forbidden" conformations yields 0.05 R for the entropy decrease in pentane, and this is too small to resolve the difficulty with the calculation of T_0 . Hence, modification of the Gibbs-DiMarzio theory to include pairwise correlations does not seem warranted.

Setting $S_c=0$ in Equation (24) and letting $v=0$, we arrive at the final expression to be compared with the set of (T_0, n) values for kinematic viscosities listed in Table III:

$$-\left[\ln \left(\frac{n+1}{2n} \right) + n^{-1} \ln 3(n+1) \right] \frac{n}{n-3} = \frac{2 \exp \left(\frac{-\epsilon}{RT_0} \right)}{1 + 2 \exp \left(\frac{-\epsilon}{RT_0} \right)} \left(\frac{\epsilon}{RT_0} \right) + \ln \left[1 + 2 \exp \left(\frac{\epsilon}{RT_0} \right) \right]. \quad (25)$$

Since Equation (25) predicts a negative T_0 for $n=5$, it is not surprising to find a large error in the prediction for $n=6$. Therefore, only the values of T_0 for $n=7$ through 20 were used in the computation of the least-squares value for ϵ , which was found to be 490.8 cal./mole. The calculated values of T_0 are shown in Table XI for this choice of ϵ . The agreement with T_0 calculated from viscosities is considered excellent, the flex energy of 490.8 cal./mole agrees with that estimated by other methods^{23,24}, and the limiting value of $T_0 = 128.8^\circ\text{K}$ as n approaches ∞ seems reasonable for linear polyethylene.

TABLE XI

Gibbs-DiMarzio Equation Using Data From Heptane to Eicosane

$$C = 490.8$$

<u>n</u>	<u>Calculated $T_{0\eta}$</u>	<u>(Observed $T_{0\eta}$ - Calculated $T_{0\eta}$)</u>
20	100.1	3.0
19	99.1	2.5
18	97.9	-1.5
17	96.6	0.3
16	95.2	-3.5
15	93.6	-1.8
14	91.8	-3.6
13	89.7	-1.6
12	87.3	-2.4
11	84.5	0.9
10	81.0	-1.6
9	76.7	4.5
8	71.0	-1.4
7	62.6	8.7

$$T_{0\eta} \text{ as } n \longrightarrow \infty = 128.8$$

Glass formation has of course not been observed in the n-alkanes because of the high rates of crystallization in these compounds, but Cohen and Turnbull³³ point out that there is reason to believe that any liquid would form a glass if cooled rapidly enough. Naturally, there is no available data on the properties of these glasses, so that we cannot independently evaluate the volume of a lattice site, or the van der Waals energy, which are parameters in the Gibbs-DiMarzio theory. Neglect of free volume is equivalent to assuming a van der Waals energy which is large compared to the flex energy. This is probably justified in the present case.

The use of a lattice model for liquids is in many respects a poor approximation, although the approximation becomes more appealing below the melting point, and especially as the glass temperature is approached. The fact that a reasonable prediction is made for heptane and all the higher homologues is a remarkable confirmation of the Gibbs-DiMarzio theory of glass formation.

4. Estimation of Flex Energy

The relative energies of different rotational conformations (conformers) are required in order to apply the Gibbs-DiMarzio theory to prediction of glass temperatures. This problem also arises in the interpretation of n.m.r. spectra, infrared spectra, chain dimensions of polymers in solution, and stress-temperature coefficients for cross-linked rubbers. Most investigations have assumed that the main contributing factor to the rotational potential is the interaction between non-bonded atoms adjacent to the bond about which rotation takes place. Mason and Kreevoy³⁴, for example, calculated the rotational potentials for substituted ethanes from the interactions between substituents. The interaction potentials were approximated by those found for rare gases having similar electronic structure to the substituent. For example, the interaction between F atoms was replaced by the potential found from the second virial coefficient of neon. A correction was added for the interactions between bond dipoles. These same potential functions were later used by Liquori, et al.³⁵, in calculating the configurational energies of isolated polymer chains.

In the calculations discussed above, the known bond lengths and angles were used. These are very difficult to predict for any given compound, yet the non-bonded interactions are quite sensitive to their exact values. Even when the known lengths and angles are used, the calculated energies are in only rough agreement with experiment. It has been suggested³⁶ that in addition to the non-bonded interactions, each bond has an "intrinsic" resistance to torsion. The contribution of this effect to rotational energies is not known.

In view of the uncertainties in the origin of the energy differences between conformers, it is not surprising that the calculated values are very unreliable. Nevertheless, even a crude estimate of conformational preferences would be of assistance in estimating flex energies, or at least in ranking structures in order of increasing stiffness. The following simple model for steric effects in alkanes was introduced by Pitzer³⁷ in 1940. The carbon-carbon bonds are assumed to be of equal length, to meet at tetrahedral angles, and to be in staggered conformations. Certain configurations can be excluded from consideration because of atom overlap. Certain others result in close approach of one or more pairs of H atoms, and these are assigned an energy a per pair. With $a = 800$ cal./mole, the model was found to account satisfactorily for entropies determined spectroscopically.

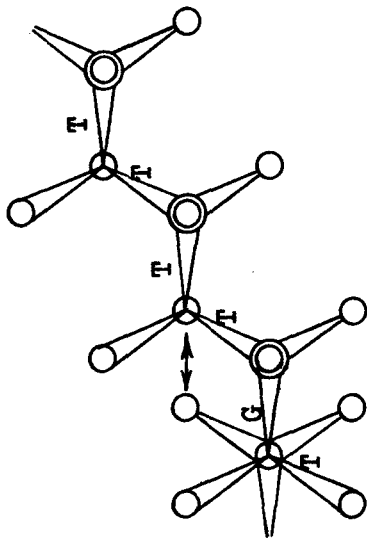
Pitzer used Fischer-Hirschfelder models to determine the number of interactions, but models can be very unwieldy when the number of atoms to be considered is large. During this program a scheme was devised for diagrammatically representing spatial configurations without atom overlap, so that the number of non-bonded nearest neighbors can be determined for the various allowed configurations, and hopefully correlated with known values of chain stiffness. The atoms are located on a tetrahedral lattice, shown in projection, with the relative levels of bonded atoms depicted by the "flying wedge" symbol. The bonds normal to the plane of the projection, so that the atoms bonded are superimposed, appear as in a Newman projection. Only staggered conformations are possible on a diamond lattice.

Schematic representations of some polymethylene chains are shown in Figure 5. The bonds are designated trans(T), gauche positive (G), or gauche negative (G') depending on the orientation of the preceding and following bonds. The all-trans sequence contains no non-bonded nearest neighbors. Rotation of one bond by 120° to the gauche position introduces one pair of non-bonded nearest neighbor H atoms (structure I). An additional G bond, either adjacent to the first (structure II), or separated from it by one T (structure III), introduces an additional pair. Hence the number of such pairs of H atoms, with interaction energy a , is simply equal to the number of G bonds. This is a justification for the use of a single value of the "flex energy" for all of the n -alkanes.

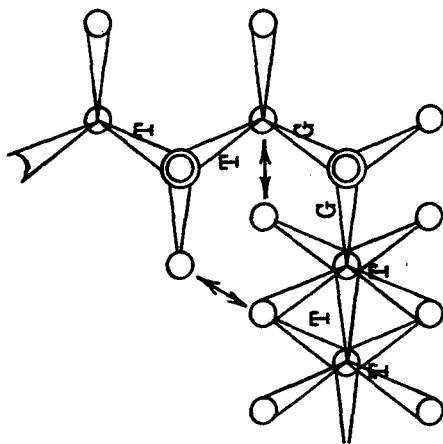
The pairs of interacting H atoms occupy adjacent positions on an open, six-membered, cyclohexane-chair-type ring, which can appear on the diagram in only two ways: on edge as in structure I or flat as in II and III (which have the additional ring on edge).

Configurations which are disallowed because of atom overlap are easily detected if the overlapping atoms are separated by six bonds, since these occupy the same position on a closed six-membered ring. More distant atoms may overlap, and it was decided to study the conditions under which this occurs. It was pointed out by Taylor³² that for chains of the type $-CX_2-$, where X is a monovalent atom, overlap of X atoms separated by six bonds occurs when any pair of successive chain bonds have the conformation GG'. Nagai and Ishikawa²⁹ determined that the next longest disallowed sequence for this type of chain is GGTGGTGG or its mirror image (formed by replacing every G with G'). This sequence results in double occupation of one site on a twelve-membered ring, as shown for undecane in Figure 5, structure IV. In general, the number of sequential rotations required to produce double occupation of a ring site equals the ring size minus four, for $-CX_2-$ type chains.

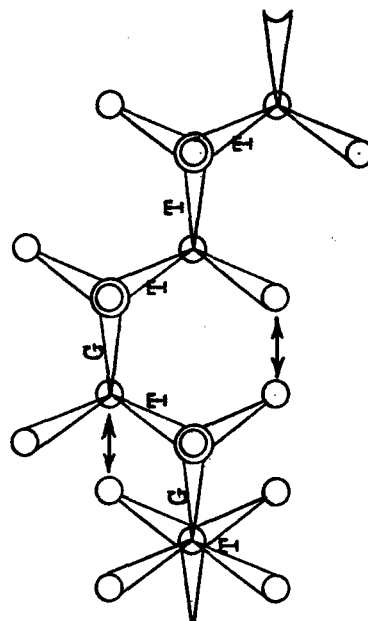
I



II



III



IV

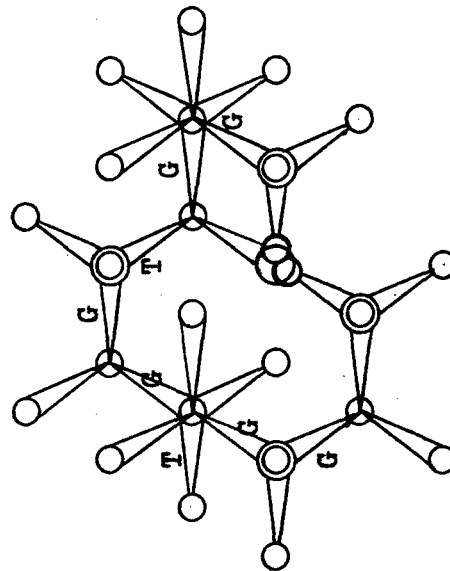


Figure 5
Intramolecular Interactions in $-CX_2-$ Chains

Overlap to close a fourteen-membered ring was found by the use of the diagrams to be possible with six different bond sequences not including GG' or GGTGGTGG. An additional six sequences which close a sixteen-membered ring were also found. The study was discontinued at this point, partly because of the publication by Smith²⁸ of the enumeration of disallowed sequences for rings of up to eighteen members, obtained with a computer. This reference should be consulted for application of the method to the problems of chain dimensions and ring stability.

The above discussion concerns only "one atom" chains of the type $-CX_2-$ where X is a single atom. "Two atom" chains such as $-CH_2-CHX-$, or $-CH_2-CX_2-$ would be of greater interest, but involve further complications: first, the pairs of side-chain atoms separated by five bonds can be of two types, H-X or H-H, and second, the steric effects resulting from bond rotation are probably no more important than the electrostatic effect resulting from the change in orientation of bond dipoles. In the case of poly(vinyl chloride) (PVC) the electrostatic interactions have been estimated by Fordham²⁹ by the use of a diamond lattice model, with the results summarized in Table XII. The eight possible configurations of the two bonds to a methylene group in isotactic (i) and syndiotactic (s) PVC result in four different electrostatic interaction energies. The steric interaction energies from Pitzer's model are included in Table XII. The most stable configuration for s-PVC is predicted to be TT, in agreement with experiment, the next highest energy configuration is TG, and the difference in energy is predicted to be $670 \pm a$. The corresponding predictions for i-PVC are TG, GG, and again a difference of $670 \pm a$.

The value of T_0 for high molecular weight PVC is seen in Table XII, Section 6 to be 42°C . As shown in Section 3, the Gibbs-DiMarzio theory predicts that $\epsilon = 3.81 T_0$ for long chains. Setting this equal to $670 \pm a$, a value of $T_0 = 316^\circ\text{K}$ corresponds to $a = 540 \text{ cal./mole}$, which is close to the H-H interaction in alkanes. The H-Cl interaction which occurs in alternate TG configurations is presumably of higher energy and does not contribute appreciably to the glass transition.

While the results of the calculation just described are in satisfactory agreement with experiment, the method has not yet been extended to other polymers because of additional problems which arise. For example, the most stable configuration of poly(vinylidene chloride) (PVCl_2) is TGTG⁴⁰. This sequence is determined by the relative orientations of three successive methylene chloride groups, requiring evaluation of steric and electronic energies of six allowed configurations on a diamond lattice. Even longer sequences should be examined in the case of polymers whose configurations have not been established, to insure that the configuration of minimum energy will be found.

TABLE XII

Electrostatic and Steric Interaction Energies in PVC (cal./mole)

	<u>TT</u>	<u>TG</u>	<u>GG</u>	<u>GG'</u>
s	140	810	1810	810
i	2780	140	810	2780
E _s	0	a	2a	∞

Another problem which has not been solved concerns the fact that polymers with two bulky substituents on the same chain atom, such as polyisobutylene, have no allowed configurations on a diamond lattice. This will require assignment of interaction energies to pairs of atoms occupying the same lattice site, to determine the configuration of lowest energy.

The problem of energy differences between rotational isomers in polymer chains has been studied by various means, all dependent on the fact that the mean square separation of the chain ends $\langle r_0^2 \rangle$ is determined by the energy differences and hence varies with temperature. In recent reviews^{21,22} of published values of $d \ln \langle r_0^2 \rangle / dT$, it was concluded that while satisfactory agreement can be reached using different methods, no satisfactory interpretation of the results exists. In particular, the theory developed by Ptitsyn²³ predicts zero or negative values of $d \ln \langle r_0^2 \rangle / dT$ for all vinyl polymers, whereas this coefficient is actually found to be positive in most cases.

The dilute solution values of $d \ln \langle r_0^2 \rangle / dT$ are open to some question, due to specific polymer-solvent interactions. Thermoelastic measurements on bulk polymers are, of course, not subject to this perturbation, and hence are probably more reliable. The flex energies computed from these measurements should agree with the Gibbs-DiMarzio estimates of flex energy from glass temperatures. However, it should be pointed out that the chain dimensions are very sensitive to correlations of rotations of neighboring bonds, and the flex energies calculated depend upon what assumptions are made concerning bond angles, rotation angles and correlations of rotations.

Table XIII shows flex energies ϵ calculated by Ptitsyn²³ from thermoelastic measurements, except for the value for isotactic poly(methyl methacrylate), which was calculated by Sakurada, et al.⁴¹ from intrinsic viscosities in different theta solvents. The corresponding flex energies from the Gibbs-DiMarzio theory shown in Table XIII were calculated from the relation

$$\epsilon = 3.81 T_0 (\infty) \quad (26)$$

as discussed in section 3. The T_0 values for polyisobutylene and natural rubber were taken from Ferry's book⁴, using the relation $T_0 = T_g - C_2$, where T_g is the reference temperature (T_g in these cases). For the silicone,

TABLE XIII

Comparison of Flex Energies \bar{E} by Different Methods

	T_0 (°K)	\bar{E} (eq. 26) (cal./mole)	\bar{E} from $d \ln \langle r_0^2 \rangle / dT$ (cal./mole)
Isotactic poly(methyl methacrylate)	277	1055	1200
Natural rubber	146	556	450
Polyethylene	129	491	500
Polyisobutylene	98	373	20
Polydimethylsiloxane	81	309	600 - 800

T_0 was estimated from T_g and C_2 reported by Barlow⁴², et al. On the assumption that C_2 is independent of tacticity, T_0 for isotactic poly(methyl methacrylate) was calculated from the glass temperature of 48° for the isotactic polymer, and $C_2 = 44^\circ$ reported by Saito, et al.⁴³ for conventional polymer. The value of T_0 for polyethylene is taken from section 3, Table XI.

The agreement seen in Table XIII for the first three polymers is encouraging, but for polyisobutylene the two methods disagree as to order of magnitude. Moreover, if Ptitsyn's²³ equation for isotactic vinyl polymers is used to calculate flex energies from the data compiled by Ciferri²² for various polyacrylates, the largest ϵ found is 97.4 cal./mole for poly(ethyl acrylate), whereas $\epsilon = 970$ from Equation (26) with $T_0 = T_g - 40 = 295^\circ\text{K}$. The atactic nature of the polymers probably accounts for the small effect of temperature on chain dimensions of the polyacrylates. That is, even in its lowest energy configuration an atactic polymer will be highly coiled due to the random arrangement of d and l units, which differ in directional properties. The higher energy states are not necessarily smaller in $\langle r_0^2 \rangle$.

5. The Cell Model of the Glass Transition

A simple kinetic model for the glass transition has been formulated using the concept of communal entropy. Communal entropy is a contribution to the total entropy of a system which exists when the molecules or other elements of the system are indistinguishable⁴⁴. The amount of communal entropy in the system is determined by the partitioning of the system into cells containing indistinguishable molecules, i.e., the degree to which the molecules in the system are interchangeable. If there are n molecules per cell, the volume per cell is $V/\frac{N}{n}$, and the number of permutations of n molecules in all N/n cells is just $(n!)^{N/n}$. Hirschfelder, Stevenson, and Eyring⁴⁵ felt that solids acquire essentially the total communal entropy on melting. This view was criticized by Rice⁴⁶ and Gurney and Mott⁴⁷. The latter authors showed that a liquid possesses almost 2/3 of the full communal entropy with only 5 molecules per cell.

If it is assumed that the main glass transition in polymers is due to motions involving s backbone atoms, where $s = 5-10$, it is possible to construct a simple model for the glass transition based on the communal entropy concept. The glass transition should occur when there are s atoms per cell.

In a system containing N polymer molecules, there will be a term in the partition function equal to $1/(\frac{n}{s})!$, where there are n chain atoms per cell. As the temperature is lowered toward T_g , this term will remain unchanged in the equilibrium partition function. However, measurements made using a finite time scale will reflect a gradual decrease in n . At T_g , $n=s$, and there will no longer be an entropy contribution from the $1/(\frac{n}{s})!$ term. Thus by producing an expression for $\frac{n}{s}$ in terms of T , it should be possible to evaluate T_g .

If we partition all of the volume into cells of n/s segments, the number of segments per cell is given by:

$$\frac{n}{s} = \frac{v \rho N}{M's}, \quad (27)$$

where

v = the cell volume

N = Avogadro's number

ρ = the polymer density

M' = the molecular weight per backbone atom.

The cell volume v is obtained as the volume of the sphere whose radius is equal to the root mean square distance travelled by each segment in time t in self-diffusion.

$$v = \frac{4}{3} \pi (6n_2tD)^{3/2} \quad (28)$$

Here D is the molecular self-diffusion coefficient and n_2 is the number of chain atoms per molecule. Equations (27) and (28) are combined:

$$\frac{n}{s} = \frac{\rho N (\frac{4}{3} \pi) (6n_2tD)^{3/2}}{M's} \quad (29)$$

This expression gives the number of segments per cell in terms of D . Unfortunately, there are very few data reported in the literature for self-diffusion of polymers. Bueche⁴⁸ has derived an expression relating D to the viscosity coefficient, η :

$$D = \frac{\rho R h^2 T}{36 M \eta}, \quad (30)$$

where

R is the gas constant, 8.314×10^7 ergs mole⁻¹ deg⁻¹,

h^2 is the unperturbed mean-square end-to-end distance in cm., and

M is the polymer molecular weight.

Substituting into Equation (29), we obtain

$$\frac{n}{s} = \left(\frac{\rho}{M'} \right)^{5/2} \left(\frac{4\pi N}{3s} \right) \left(\frac{tRh^2 T}{6\eta} \right)^{3/2} . \quad (31)$$

The viscosity is well represented by the Fulcher² equation:

$$\log \eta = \log A + \frac{B}{T - T_0} . \quad (32)$$

The appropriate substitution is made to reach the final expression:

$$\frac{n}{s} = \left(\frac{\rho}{M'} \right)^{5/2} \left(\frac{4\pi N}{3s} \right) \left(\frac{tRh^2 T}{6A \exp \left[\frac{2.303B}{T - T_0} \right]} \right)^{3/2} . \quad (33)$$

The condition for T_g is that $\frac{n}{s} = 1$. Thus, at T_g

$$0 = \frac{5}{3} \log \left(\frac{\rho}{M'} \right) + \frac{2}{3} \log \frac{4\pi N}{3s} + \log \frac{tRh^2 T_g}{6} - \log A$$

$$-B \left[\frac{1}{T_g - T_0} \right] . \quad (34)$$

Equation (34) is a transcendental equation and therefore a solution cannot be obtained by ordinary algebraic methods. However, a solution is obtained rapidly by using a self-consistent iterative method. Since $T_g = 0$ (300°K), it follows that $T_g \gg \log T_g$. Therefore, if an approximate value of T_g is used in the $\log T_g$ term, the equation becomes linear in T_g . This equation is solved for T_g , and then the solution is used as the estimate in the $\log T_g$ term. The process is repeated until the solution and estimate agree within the desired tolerance. Ordinarily no more than two iterations are required.

Although Equation (34) is the result of a rather simple derivation, it may be seen readily that it is in qualitative agreement at least with current theories of the glass transition. The equation predicts that T_g will increase with the monomer molecular weight and decrease with increasing time scale of the experiment, approaching a lower limit of T_0 as t approaches infinity. The latter prediction agrees with the Gibbs and DiMarzio⁵ theory of a lower limit to T_g at an equilibrium second-order transition temperature, T_2 . The inverse relationship between T_g and the end-to-end distance h^2 in Equation (34) can be disturbing unless one considers the effect of the viscosity (see Equation 31). It is well-known that in the high-molecular weight region⁵

$$\langle h^2 \rangle_0 = AM \quad (35)$$

and

$$\eta = A'M^{3.4}. \quad (36)$$

Thus the net result is a positive dependence of T_g on M .

A test of the theory was made using Miller's¹ results for two low-molecular-weight polystyrene fractions, for the choices $s=5$, $t=1000$ sec., and $\rho=1.0$ g/cc. The results are given below in Table XIV.

TABLE XIV

Glass Temperatures of Polystyrene Calculated with Equation (34)

<u>M_{vis}</u>	<u>T_g, °K, Exptl.</u>	<u>T_g, °K, Eq. (34)</u>	<u>Error, °K</u>
6650	350	353	+3
3041	337	336	-1
1675	313	319	+6

Viscosity-temperature data based on a number of polymers were fitted to an equation of the form of Equation (12),

$$\log \eta_T = \log A' + \frac{B}{T - T_0'} , \quad (12)$$

in order to obtain activation parameters. (This will be discussed in more detail in the next section.) The results were used to calculate glass temperatures for these polymers after Equation (34) was modified to conform with Equation (12):

$$0 = \frac{5}{3} \log \left(\frac{P}{M'} \right) + \frac{2}{3} \log \frac{4\eta N}{3s} + \log \frac{tRh^2 T_g^2}{6} - \log A' - B'/(T_g - T_0'). \quad (37)$$

Glass temperatures were calculated with $t=1000$, $s=5$, and $\rho=1$ as before. All values of h^2 in this work were taken from Kurata and Stockmayer's⁴⁹ values, which are based on intrinsic viscosities. The results are given in Table XV.

In general it may be seen that the results are in good agreement with experiment. This is especially gratifying in view of the fact that the lowest measurement temperature was often well above the experimental glass temperature. In the case of poly(decamethylene adipate), for instance, the glass temperature is predicted with an error of 6°K from a point 144°K above it.

During this study it was found that virtually all recent publications concerned with transitions in polyisobutylene use the Flory-Fox equation¹⁵,

$$T_g, ^\circ\text{C} = -63 - 6.9 \times 10^4/M, \quad (38)$$

to express the relationship between T_g and molecular weight. Equation (38) is in fact based on the measurement of T_g for a single polymer sample⁵³, plus certain free-volume considerations. The few other values of T_g appearing in the literature do not conform closely to this equation, therefore, only one experimental value of T_g is given in Table XV for polyisobutylene.

It was demonstrated in this program that the use of kinematic viscosity instead of absolute viscosity in the Fulcher equation results in a better fit of the experimental data:

$$\log \eta = \log \rho + \log A + \frac{B}{T-T_0} \quad (39)$$

This of course results in changes in each of the three parameters A, B, and T_0 . Substitution of Equation (39) into Equation (31) leads to the following expression for T_g :

TABLE XV

T_g Values Computed Using Equations (12) and (31)

Polymer	Ref.	$\bar{M}_n \times 10^4$	Temp. Range of Measurement, °K	T _g , °K		Error
				Exptl.	Calc.	
Polystyrene	50	1.93	403 - 490	362	363	+1
	50	1.33	403 - 490	359	359	0
	50	0.665	393 - 490	350	354	+4
	50	0.359	373 - 490	348	345	-3
Polyisobutylene	51	48.0	281 - 490	-	223	-
	51	8.00	264 - 490	-	196	-
	51	5.76	383 - 490	-	169	-
	51	1.29	329 - 490	-	203	-
	51	0.538	260 - 490	197*	201	+4
Poly(decamethylene adipate)	51	0.0755	238 - 490	-	200	-
Poly(diethylene adipate)	52	0.4510**	355 - 475	217 ⁵⁴	211	-6
	52	0.0900**	273 - 440	227 ⁵⁴ , 205 ⁵⁵	216	0***

* Reported in Ref. 53 for $\bar{M}_n = 4900$.

** Number-average molecular weight.

*** The experimental value of T_g was taken as the average of the two literature values.

$$0 = \frac{2}{3} \log \frac{4\pi\eta\rho}{3s} - \frac{5}{3} \log M' + \log \frac{tRh^2T_g}{6} - \log A$$

$$-B \left[\frac{1}{T_g - T_0} \right] \quad (40)$$

Equation (40) was tested using constants for Equation (39) previously determined (see Table III) on smoothed n-alkane kinematic viscosity data⁷.

Values of T_g were calculated using Equation (40) for a group of n-alkanes ranging from Z equals 7 to 64 carbon atoms with $t=100$ seconds and $s=5$. The calculated values are presented in Table XVI. The values were plotted according to the method of Fox and Loshaek^{5,6},

$$\frac{1}{T_g} = \frac{1}{T_g^\infty} + \frac{K}{M}, \quad (41)$$

to yield T_g^∞ , defined as the glass transition temperature at infinite molecular weight. The plot showed an even-odd alternation (see Table XVI) which made it difficult to see trends in the data. This effect was removed by plotting average values for each pair of data points,

$$\left(\frac{1}{Z} \right) = \frac{\left(\frac{1}{Z} \right)_n + \left(\frac{1}{Z} \right)_{n+1}}{2},$$

$$\left(\frac{1}{T_g} \right) = \frac{\left(\frac{1}{T_g} \right)_n + \left(\frac{1}{T_g} \right)_{n+1}}{2} \quad (42)$$

where n is an odd integer. The result is shown in Figure 6.

TABLE XVI

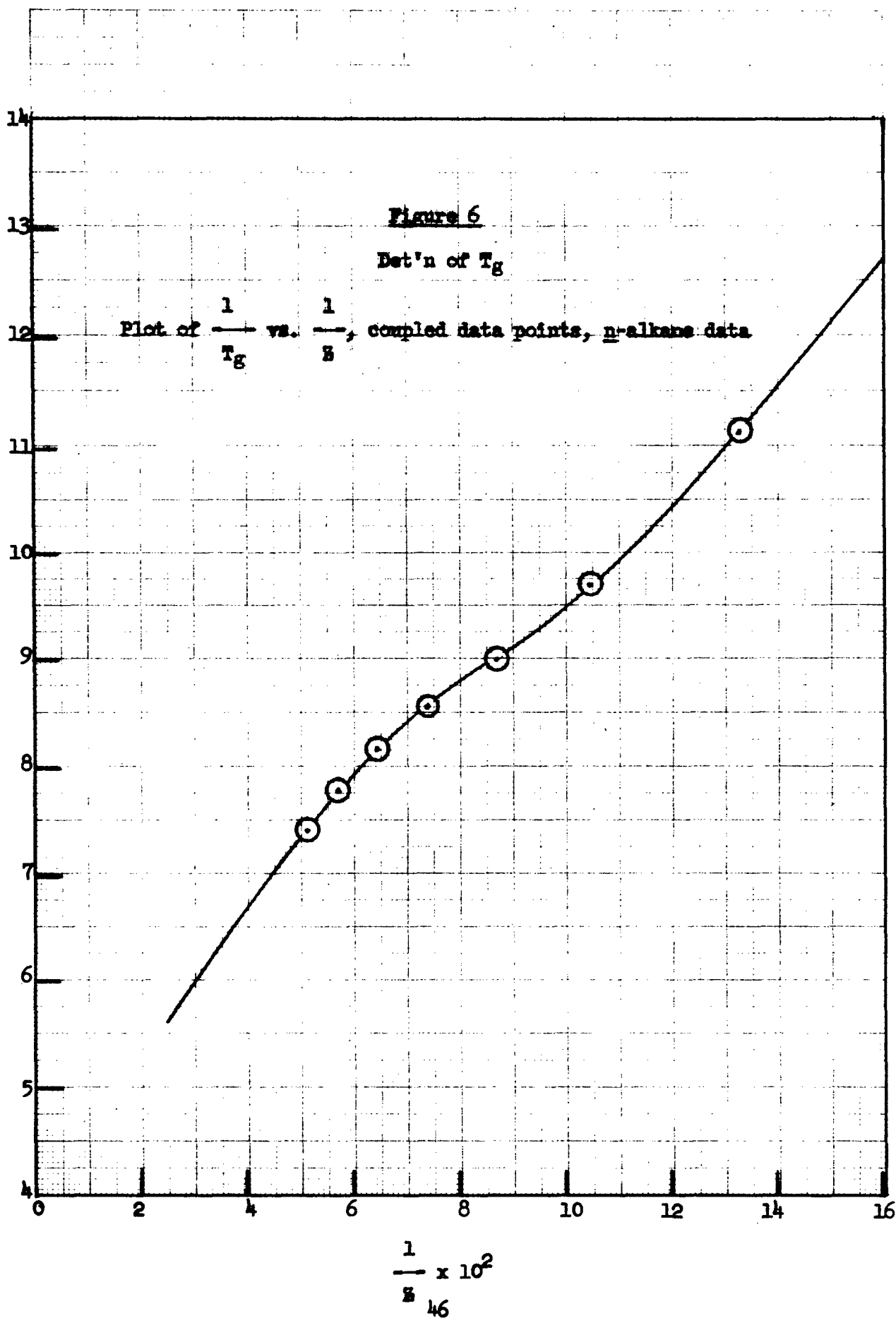
Tg Values Computed for n-Alkanes Using Equation (39)

<u>Z</u>	<u>Tg, °K</u>	<u>Tg-To</u>
5	67.9	13.4
6	75.0	16.1
7	88.4	17.1
8	89.4	20.3
9	102.1	20.9
10	102.9	23.5
11	109.9	24.5
12	111.4	26.5
13	115.6	27.5
14	117.2	29.0
15	121.5	29.7
16	122.6	30.9
17	127.9	31.0
18	128.5	32.1
19	133.6	32.0
20	135.8	32.7
64*	175*	41.*

* Based on data of A. K. Doolittle, Ref 8. Equation (39) parameters shown in Table III.



$$\frac{1}{T_g} \times 10^3$$



Extrapolation of $1/T_g$ to $\frac{1}{Z} = 0$ cannot be performed accurately because of the curvature of the function and the lack of higher alkane data. It does appear that $1/T_g^\infty$ will be near 4×10^{-3} , however, giving a value of T_g^∞ of approximately 250°K. This corresponds closely to the β transition range in polyethylene, which lies near 250°K.

6. Transition State Thermodynamics in the Glass Transition Region

In the study of the n-alkanes described in Section 5, it was observed that $(T_g - T_0)$ increases with molecular weight. In an effort to explain this, we examined the relationship between the Fulcher equation and the simple Arrhenius equation for the viscosity of liquids. According to the two expressions, the following equality exists:

$$\log \eta = \log A + B/(T - T_0) = \log A' + \frac{E_\eta}{2.303 RT} \quad (43)$$

Take the derivative of $\log \eta$ with respect to $1/T$ and rearrange to obtain

$$E_\eta = 2.303 RB \left(\frac{T}{T - T_0} \right)^2, \quad (44)$$

the activation energy in terms of the Fulcher parameters. At the glass temperature this becomes

$$E_g = 2.303 RB \left(\frac{T_g}{T_g - T_0} \right)^2. \quad (45)$$

The use of kinematic viscosity rather than absolute viscosity leads to a complication. If kinematic values are used, E_g in Equation (45) gives the kinematic value of E_g . Differentiation of Equation (39) yields the result

$$E_{g, \text{ absolute}} = E_{g, \text{ kinematic}} + 2.303 R \alpha T_g^2, \quad (46)$$

where α is the expansion coefficient. α is equal to $1 \times 10^{-3} \text{ deg}^{-1}$ to a good approximation for the n-alkanes, leading to a correction term of 0.04 kcal. for a glass temperature of 100°K. The calculated values of $E_{g, \text{ kin.}}$ and $E_{g, \text{ abs.}}$ are given in Table XVII.

TABLE XVII

Activation Energies for n-Alkanes

<u>Number of Carbon Atoms</u>	<u>E_g kin., kcal.</u>	<u>E_g abs., kcal.</u>	<u>$\left(\frac{E_g \text{ abs.}}{T_g} \right) \times 10^2$</u>
5	3.59	3.61	5.32
6	4.01	4.04	5.39
7	4.80	4.84	5.48
8	4.92	4.96	5.52
9	5.65	5.70	5.58
10	5.75	5.80	5.64
11	6.17	6.23	5.67
12	6.26	6.32	5.67
13	6.54	6.60	5.71
14	6.66	6.72	5.73
15	6.92	6.99	5.75
16	7.01	7.08	5.77
17	7.34	7.41	5.80
18	7.38	7.46	5.81
19	7.70	7.78	5.82
20	7.82	7.90	5.82
64*	10.3*	10.4*	5.95*

* Based on data of A. K. Doolittle, Ref. 8. Equation (14) parameters shown in Table III.

Examination of the data revealed that the ratio $E_g \text{ abs.}/T_g$ is nearly constant over the range of alkanes studied, and appears to be approaching a truly constant value at higher molecular weights.

This treatment was not based on experimental values of T_g . Therefore, a study of literature data on the temperature dependence of viscosity and dielectric relaxation time for a variety of polymers was initiated. The bulk of the viscosity data was obtained by Fox and Flory^{50,51}. The dielectric dispersion data was published by Saito⁴³.

It has been amply demonstrated in the literature that the temperature dependence of the shear viscosity and dielectric relaxation time of amorphous polymers can be expressed over broad temperature ranges above the transition region by the Fulcher equation^{57,59,60}. Miller⁵⁷ has shown that the well-known WLF equation is mathematically equivalent to the Fulcher equation. Cohen and Turnbull³³ have derived a slightly different relationship for self-diffusion using a statistical mechanical approach:

$$\log D = \log A + \log T^{1/2} + \frac{B}{T-T_0} . \quad (47)$$

The utility of this equation has been discussed by Miller⁵⁷. Angell⁵⁸ has had considerable success with it in describing the temperature behavior of self-diffusion and electrolytic conductance in glass-forming molten salt mixtures. It was shown in Section 1 that another relationship,

$$\log \eta = \log A - \log T + \frac{B}{T-T_0} , \quad (48)$$

fits n-alkane data better than the Fulcher equation, as indicated by much lower variance estimates in least-squares calculations. Equation (48) is a very convenient one for the study of the transition state. This will now be demonstrated.

The Eyring⁹ theory of the transition state defines the free energy of activation, i.e., the free energy difference between the initial state and the transition state in the expression

$$\log k_2 = \log \frac{K k}{h} + \log T - \frac{\Delta G^\ddagger}{2.303 RT}, \quad (49)$$

where k_2 is the reaction rate, K is a transmission factor usually taken as unity, which accounts for the fact that not all species reaching the transition state actually decompose to products, and the other symbols have their usual meanings. This theory, although originally conceived to describe chemical reactions, has frequently been applied to other irreversible phenomena including viscous flow⁹ and dielectric relaxation⁶¹.

The description of viscosity and dielectric relaxation time requires the inversion of Equation (49), because these properties are inversely proportional to rate or frequency of motion:

$$\log \eta = \log A - \log T + \frac{\Delta G^\ddagger}{2.303 RT}, \quad (50)$$

Here the $\frac{h}{K k}$ term is simply called A , indicating that it is a constant.

It is felt that A should be a constant independent of temperature, since the only variable is K and this should depend only on the nature of the polymer.

Comparison of Equation (48) and (50) indicates that as T approaches infinity, the two equations become identical, with $\Delta G^\ddagger/2.303 R = B$. This means that the values of A in both equations are the same, leading to the following result for all temperatures:

$$\Delta G^\ddagger = \frac{2.303 RBT}{T-T_0}. \quad (51)$$

The activation energy E_η (or E_γ) is obtained by differentiation of $\log \eta$ with respect to $\frac{1}{T}$, giving

$$E_\eta = RT + 2.303 RB \left(\frac{T}{T-T_0} \right)^2. \quad (52)$$

Finally, by making the usual assumption that the activation enthalpy ΔH^\ddagger is related to $E\eta$ by

$$\Delta H^\ddagger = E\eta - RT, \quad (53)$$

we can obtain the entropy of activation:

$$\Delta S^\ddagger = \frac{E\eta - \Delta G^\ddagger - RT}{T}. \quad (54)$$

Equations (51) and (52) show that the activation energy and free energy increase with decreasing temperature, approaching infinity as T approaches T_0 . It can be shown that the same is true of the entropy of activation. Combination of Equations (51), (52), and (54) yields the expression,

$$\Delta S^\ddagger = \frac{2.303 RB}{T-T_0} \left[\frac{T}{T-T_0} - 1 \right], \quad (55)$$

which clearly goes to infinity at T_0 .

The viscosity and relaxation time data^{43,50-52} were used to evaluate the parameters A , B , and T_0 in Equation (48) employing a non-linear least-squares method. The transition state functions $E\eta$ (and $E\gamma$), ΔG^\ddagger , and ΔS^\ddagger were then computed at the glass temperature.

Tables XVIII and XIX give the results of these calculations.

Eyring⁹ derived an alternate expression for the free energy of activation in viscous flow by assuming that the molecules of a liquid move from one equilibrium position to another under the influence of an applied force:

$$\Delta G_V^\ddagger = 2.303 RT [\log \eta + \log V - \log Nh]. \quad (56)$$

TABLE XVIII

Transition State Parameters at T_g for Dielectric Relaxation, Based on Saito's⁴³ Data

Polymer	$M_{vis} \times 10^{-4}$	$T_g, ^\circ K$	$\log \tau_g^*$	$-\log A$	B	T_0	$s^2 \times 10^{4**}$	$E_T, \text{kcal.}$	$\Delta G^\ddagger, \text{kcal.}$	$\Delta S^\ddagger, \text{eu}$
PEMA	-	289.2	0.21	8.65	905.1	209.2	5.4	54.6	14.9	135
PEMA	-	323.2	3.45	8.43	854.5	263.8	8.9	116.2	21.3	292
PMMA	110	380.2	1.63	11.00	666.2	336.3	1.5	228.9	26.4	531
	54	377.2	1.71	12.55	846.6	326.9	26.4	218.1	28.8	500
	33	373.7	2.09	9.52	527.6	336.5	11.2	243.9	24.2	586
	15	371.7	1.58	12.90	910.1	318.3	3.1	202.1	29.0	464
	8.5	366.2	2.27	12.86	900.6	315.3	6.5	213.7	29.6	501
PVC	17.4	358.7	0.95	11.82	666.8	315.2	17.5	207.9	25.1	508
	10.1	357.2	1.00	13.09	815.6	308.2	7.1	198.6	27.2	478
	7.6	356.2	0.79	13.15	837.6	305.4	3.0	188.7	26.8	453
	5.8	354.2	0.89	13.59	898.7	301.4	3.4	185.4	27.6	444
	4.57	353.4	0.79	12.77	799.6	303.7	0.12	183.7	26.0	447
	3.62	351.7	0.86	13.29	864.8	299.9	2.9	182.8	26.9	441
PVAc	52.3	304.2	4.36	10.38	738.7	261.3	7.6	170.3	23.9	479
	26.1	303.2	4.99	9.53	620.6	266.7	25.9	196.3	23.6	567
	18.8	303.2	4.68	9.65	633.7	265.6	16.2	187.9	23.3	541
	11.2	303.2	4.56	10.47	746.0	260.6	8.8	173.3	24.3	489
	3.95	302.2	5.13	9.25	587.0	267.4	31.2	202.8	23.3	592

* τ_g calculated using Equation (48) and T_g values of Saito.

** Variance estimate, least squares fit.

TABLE XIX

Transition State Parameters at T_g for Viscous Flow

Polymer	$M_{vis} \times 10^{-4}$	$T_g, ^\circ K$	$\log \eta_g$	$\log A$	B	T_0	$s^2 \times 10^4$	$E_T, kcal.$	$\Delta G^\ddagger, kcal.$	$\Delta S^\ddagger, eu$	Ref.
PS	1.930	362	13.91	0.5437	645.3	321.5	69.0	236.2	26.4	578	50
	1.330	359	13.47	0.3249	645.9	317.3	72.0	222.4	25.8	546	50
	0.665	350	15.18	0.2088	588.7	316.4	50.0	292.5	28.1	753	50
	0.359	348	11.41	-0.2067	604.7	305.3	19.9	183.6	22.5	461	50
PIB	48.0	-	-	5.839	952.6	142.6	15.1	-	-	-	51
	8.0	-	-	2.208	1360.6	103.0	1.13	-	-	-	51
	5.76	-	-	0.956	1888.0	47.1	3.58	-	-	-	51
	1.29	-	-	0.253	1167.9	128.5	4.03	-	-	-	51
	0.54	197	13.990	-0.507	1096.5	131.7	18.26	46.0	15.1	155	51
	0.076	-	-	-0.0148	921.1	136.6	43.1	-	-	-	51
Decamethylene Adipate	0.451*	217	11.216	1.6319	460.1	178.4	0.258	44.9	11.8	151	52
Diethylene Adipate	0.090**	216**	12.674	0.364	374.9	190.4	0.131	122.0	14.5	496	52

* Number-average molecular weight.

** Average of two literature values.

The subscript, v, indicates that the free energy defined by Equation (56) is being used. By comparing activation enthalpies of linear polyesters with heats of vaporization of analogous simple esters, Eyring concluded that the molar volume V of a moving polymer segment is about 500 cm³. In order to follow his theory through, we shall assume the same value.

Equations (56) and (48) may be combined to yield

$$\Delta G_V^\ddagger = 2.303 RT [\log A - \log T + \frac{B}{T-T_0} + \log V - \log Nh]. \quad (57)$$

Now ΔG_T^\ddagger , the free energy defined in Equation (51), is taken out of the brackets to give

$$\Delta G_V^\ddagger - \Delta G_T^\ddagger = 2.303 RT [\log A - \log T + \log V - \log Nh]. \quad (58)$$

Equation (58) is simplified numerically by substituting the value of $\log V$ and $\log Nh$,

$$\Delta G_V^\ddagger - \Delta G_T^\ddagger = 2.303 RT [\log A - \log T + 5.098]. \quad (59)$$

Values of ΔG_V^\ddagger and ΔS_V^\ddagger computed using Equation (59) are shown in Table XX. It may be seen that the free energy values are somewhat higher, and the entropy values slightly lower than those in Table XIX. Thus, the results are still basically the same as before. Therefore, the discussion which follows applies to both sets of results.

It is quite obvious that in contrast with the n-alkane results in Table XVII the ratio of activation energy to temperature is not a constant at the glass temperature, except possibly within the same polymer series.

Several comments on the nature of the transition state near the glass temperature can be made.

TABLE XX

Transition State Parameters at T_g Based on Eyring Viscosity Theory

<u>Polymer</u>	<u>$M_{vis} \times 10^{-4}$</u>	<u>G_v^\ddagger, kcal.</u>	<u>S_v^\ddagger, eu</u>
PS	1.930	31.5	564
	1.330	30.5	533
	0.665	32.5	741
	0.359	26.2	451
PIB	0.54	17.2	143
Decamethylene Adipate	0.451	16.2	129
Diethylene Adipate	0.090	17.6	481

First, the activation energy is quite large, around 200 kcal., at the glass temperature, except for those polymers with very low glass temperatures. It is obvious from this that a rather large region in the polymer must be involved in motions leading to the glass-transition.

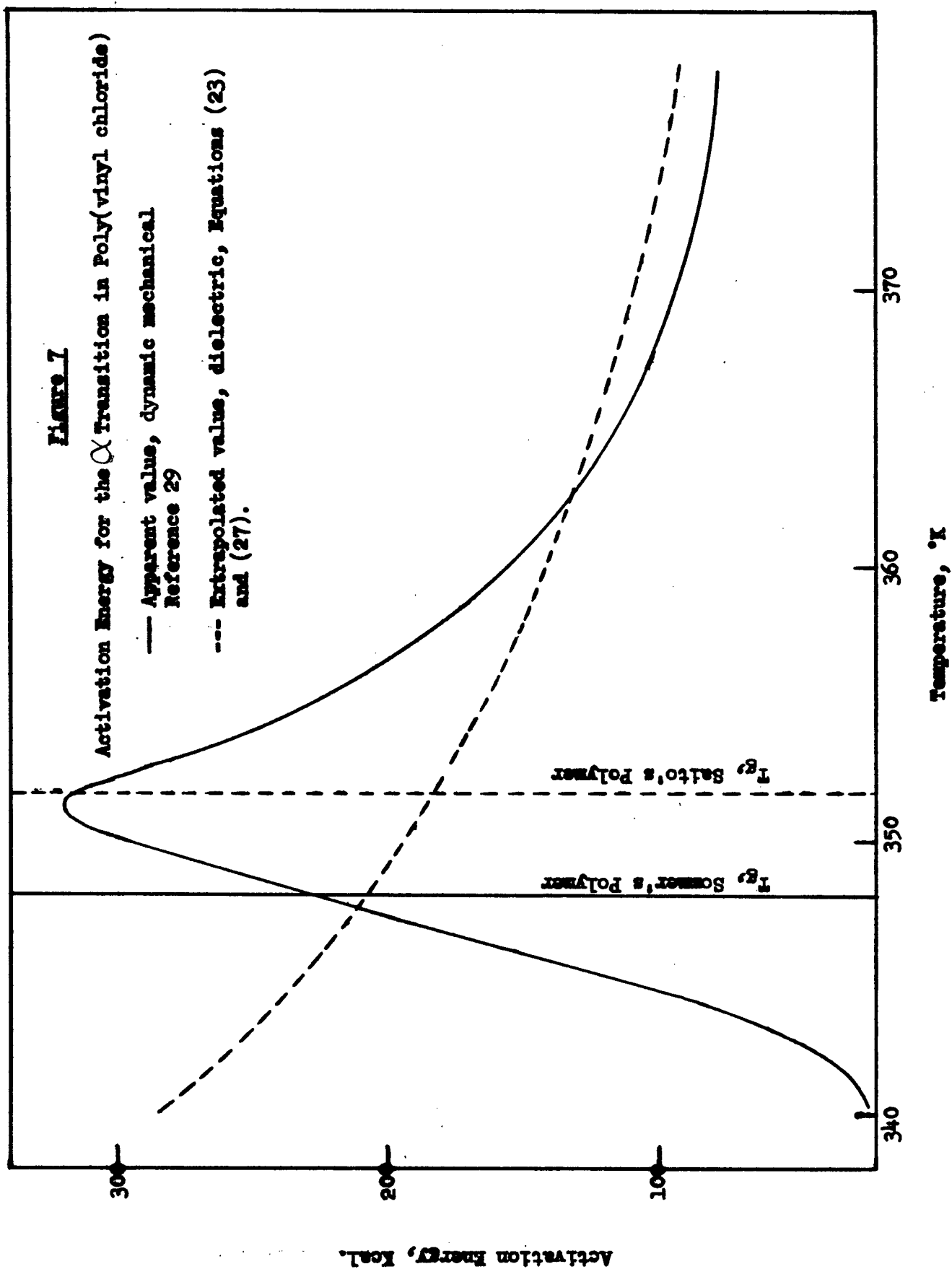
The activation entropy is large and positive in every case. This indicates that the formation of the transition state requires considerable disordering of the polymer in the transition region. At least two explanations for this are possible. First, the size of the volume element affected by the motion of a particular group may increase, and second, there may be an increase in short-range order in the neighborhood of the transition temperature necessitating the creation of relatively more disorder to reach the transition state. It is likely that both effects contribute to the large positive entropy of activation.

The free energy of activation at the glass temperature was found to be positive in every case. The variation in this property was much less than that of the entropy or activation energy, ranging from a value of 12 for poly(decamethylene adipate) to 30 for PMMA.

A rather obvious result of this work is the close correspondence between the α dielectric dispersion process and the viscous flow process above T_g . Although both processes were not studied for any given polymer, the activation energies seem to be approximately equal for polymers with the same T_g in either process.

This correspondence between dielectric and mechanical properties has been observed before⁶². These results supply additional evidence for the equivalence of dielectric and mechanical relaxation phenomena. Although the similarity between the response of a dipole to an alternating electric field and the response of a polymer to a mechanical stress may not be apparent at first, it is easily understood when we consider the size of the region involved in the response of a single dipole. The magnitude of the activation energy at T_g is a clear indication that this region is quite large, involving coordination with seemingly unrelated portions of the polymer. This is qualitatively similar to the coordination required for mechanical relaxation.

It has been observed by several workers^{63,64} that the activation energy for the α relaxation process has a maximum value near the dilatometric glass transition temperature. Figure 7 shows the results obtained by Sommer⁶³ from dynamic mechanical measurements on poly(vinyl chloride) with an average molecular weight of 35,000. Superimposed is the activation energy curve predicted by Equation (48) and (52), based on Saito's⁴³ dielectric data on poly(vinyl chloride) with M_{vis} equal to 36,000.



It can be seen that the value of the activation energy at T_g is somewhat higher for the mechanical process than the dielectric process. This is not unreasonable, especially in the case of polymers, where the coordination required for motion of a single dipole should be more localized than that required for over-all mechanical relaxation. If this rationale is correct, the dielectric and mechanical activation energies should be nearly identical for small polar molecules. Davidson and Cole⁶⁰ found this to be so in the case of *n*-propanol and glycerine. Actually these authors evaluated the Fulcher equation constants for dielectric relaxation time and viscosity and found B and T_0 to be virtually identical for the two processes, which of course indicates equal activation energies.

Below the glass temperature the experimental (mechanical) value of the activation energy declines, but the calculated value continues to increase and will in fact go to infinity at T_0 .

How can the discrepancy between experimental observation and calculation be explained? Fox and Flory¹⁵ suggested that the decrease in activation energy was due to a condition of constant free volume below T_g . A more satisfactory explanation has been proposed by Saito⁴³. He found that the activation energy for dielectric relaxation can be increased in the transition region by cooling the sample to the measurement temperature more slowly. He proposed that the decrease in activation energy is caused by the non-equilibrium nature of the sample below T_g . In other words, the time required for equilibration below T_g is so long that the polymer behaves as though it were still at some higher temperature.

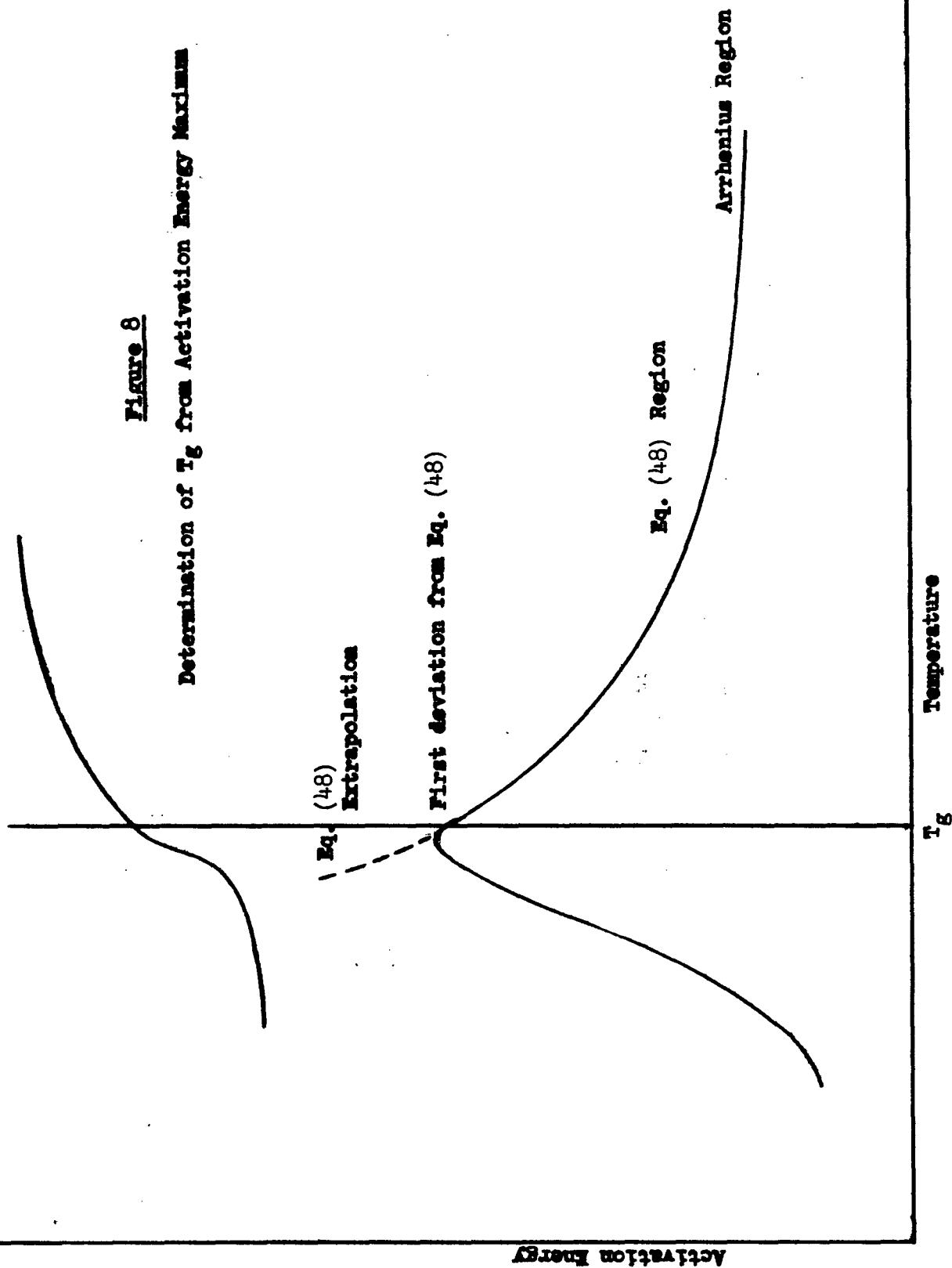
The activation energy peak in Sommer's plot occurs at 351°K, which is within the range reported in the literature for the T_g of poly(vinyl chloride). It would appear on the basis of the discussion above that the position of the activation energy maximum corresponds closely to the glass temperature determined dilatometrically. The glass temperature measured in this way depends only on the sample and not on an arbitrary frequency of measurement.

An illustration of the proposed method is shown in Figure 8. The glass temperature is shown in the figure as the first temperature at which the experimental data deviates from Equation (48), since this is the first indication of a non-equilibrium condition in the polymer. A hypothetical maximum-loss frequency curve is also shown in Figure 8, to show that it is not absolutely necessary to calculate and plot the activation energy in order to determine T_g .

It would be of interest to study the β transitions of several polymers in order to see if there is a corresponding peak in the activation energy. If such a peak exists, it should lead to some new thoughts concerning the nature of the β transition, particularly regarding free volume. Similarly it should be determined if there is a second maximum in the activation energy of the β process in the neighborhood of T_g .

Figure 8

Determination of T_g from Activation Energy Maximum



VII. Intermolecular Interactions

The forces of interaction between molecules play an important role in the equilibrium and transport properties of liquids, and hence also in the transition to other states such as the glass. It is not surprising, therefore, to find that many theories and empirical correlations related to the glass transition temperature are expressed in terms of some measure of intermolecular attraction, such as the cohesive energy density, the hole energy or the thermal coefficient of expansion of free volume. The pressure coefficients in Table VI are also a measure of intermolecular forces. It would be desirable to be able to predict the effects of molecular structure on intermolecular interactions.

A correlation proposed by Small⁶⁵, derived from the van der Waals equation, treats $(EV)^{1/2}$ as a constitutive property, E being the cohesion energy per mole and V the molar volume. Since E is a function of temperature, an attempt was made to adapt this correlation to the prediction of the Antoine parameter B_p , which is temperature-independent, by means of the relation

$$E = 2.303R B_p T^2 / (T - T_0)^2 - RT. \quad (60)$$

The values of the Antoine constants B_p and T_0 selected by API Project 44 for the n-alkanes⁷ were submitted to the Mathematical Analysis Group to test the function

$$\left[2.303 R B_p T^2 / (T - T_0) - RT \right]^{1/2} V^{1/2} = a_1 n + b_1$$

which follows from Equation (60) and the additivity of $(EV)^{1/2}$. The values of the adjustable parameters a_1 and b_1 were chosen so as to minimize the sum of squares of the deviations in B_p . As shown in Table XXII, the fit to the data is quite poor, which may be due to the approximations inherent in Equation (60), rather than shortcomings in Small's correlation.

It was thought that $(B_p V)^{1/2}$ might be an additive property, by analogy, but this is not the case. However, it has been found that

$$(B_p V)^{0.7240} = 835.59 n + 732.14 \quad (62)$$

gives a very good fit, as seen in Table XXIII. A number of empirical correlations for the Antoine constants were studied, and the results

Table XXI

Constants for the n-Paraffin Hydrocarbons*

n	m/d	d	T _o	B _p
3	89.48	0.49281	25.16	813.20
4	101.43	0.57305	33.16	945.90
5	116.104	0.62143	41.16	1064.63
6	131.598	0.65486	48.794	1171.530
7	147.456	0.67957	56.260	1268.115
8	163.530	0.69854	63.643	1355.126
9	179.670	0.71386	71.541	1428.811
10	195.905	0.72631	78.680	1501.268
11	212.217	0.73658	85.138	1572.477
12	228.579	0.74522	92.849	1625.928
13	244.924	0.75276	98.877	1689.093
14	261.312	0.75923	105.626	1739.623
15	277.698	0.76494	111.869	1789.658
16	294.083	0.77002	118.632	1831.317
17	310.51	0.77445	123.140	1880.61
18	326.93	0.77847	128.63	1920.60
19	343.36	0.78207	133.56	1961.6
20	359.83	0.78525	139.96	1994.0

* Values taken from Reference 7

Table XXII

$$B_p = \left[\frac{d}{m} (a_1 n + b_1)^2 + 592.48 \right] \left[\frac{(298.15 - T_o)^2}{406,750} \right]$$

$$a_1 = 1.5845 \times 10^2$$

$$b_1 = 1.7165 \times 10$$

<u>n</u>	<u>Calculated B_p</u>	<u>(Observed B_p - Calculated B_p)</u>
3	605.24	207.96
4	823.53	122.37
5	1012.43	52.20
6	1178.736	-7.206
7	1322.793	-54.678
8	1444.803	-89.677
9	1538.378	-109.567
10	1620.845	-119.577
11	1694.582	-122.105
12	1730.077	-104.149
13	1777.412	-88.319
14	1796.684	-57.061
15	1811.130	-21.472
16	1802.062	29.255
17	1826.68	53.93
18	1820.97	99.63
19	1817.6	144.0
20	1772.1	221.9

Table XXIII

$$B_p = \frac{d}{m} [a_2^n + b_2]^{c_2}$$

$$a_2 = 8.3559 \times 10^2$$

$$b_2 = 7.3214 \times 10^2$$

$$c_2 = 1.3813$$

<u>n</u>	<u>Calculated B_p</u>	<u>(Observed B - Calculated B)_p</u>
3	789.03	24.17
4	955.72	-9.82
5	1080.32	-15.69
6	1184.205	-12.675
7	1274.868	-6.753
8	1355.915	-0.789
9	1430.191	-1.380
10	1498.587	2.681
11	1562.112	10.365
12	1621.634	4.294
13	1678.130	10.963
14	1731.577	8.046
15	1782.607	7.051
16	1831.474	-0.157
17	1878.14	2.47
18	1923.09	-2.49
19	1966.4	-4.8
20	2008.0	-14.0

are shown in Tables XXIV to XXVII. The three predictors for T_0 are roughly equivalent, and that shown in Table XXVII is probably the best choice

$$(T_0/d)^{1.3248} = 46.879 n + 27.514 \quad (63)$$

Equation (62) shows that a constant increment of 835.59 in $(B_p V)^{0.724}$ results from an increase in chain length of one atom. Rearranging, and defining a new parameter $Q = (B_p V)^{0.724}/835.59$, we have

$$Q = n + 0.876 \quad (64)$$

for n-alkanes. Q was calculated for some branched alkanes, using values of B_p and V tabulated by API Project 44.⁷ It was found that the presence of a branch reduced the value of Q by about 0.15 for each side group s , compared with the expected value for the normal isomer of the same n . To illustrate the magnitude of the deviations from this rule, the values of $Q - n + 0.15s - 0.876$ are listed in Table XXVIII.

The values for 2,3-dimethyl isomers are omitted from Table XXVIII because they were higher by an average of 0.037 than those calculated from $Q - n + 0.15s - 0.876$. While the deviation is very small, it seemed to be consistent, so a number of other compounds with vicinal side chains were studied. The average deviation for 12 compounds with vic side chains, and for which B_p was reported to at least 0.1° , was 0.035 for each pair of vic side groups v . To illustrate the adherence to this rule, values of $Q - n + 0.15s - 0.035 v - 0.876$ are listed in Table XXIX.⁶⁶ Data for the last eight compounds in the table are from Driesbach.

The largest errors in the use of $Q = n - 0.15s + 0.035 v + 0.876$ occur in those compounds where B_p is reported only to the nearest degree, and are therefore the least reliable. The worst case is 3-isopropyl-2-methylhexane, Table XXIX, for which the calculated $B_p = 1474^\circ$, an error of 45° or 3%. Of those compounds for which B_p is reported to better than 0.1° , the largest error occurs with 2-methylheptane, for which the calculated $B_p = 1315.96^\circ$, an error of 21.51° or 1.6%. The most convincing evidence, however, of the precision of this correlation, is the fact that it is able to distinguish a third-order effect, that due to the placement of side chains on adjacent carbon atoms.

It is recommended that these correlations for the Antoine constants of alkanes be extended to include other classes of compounds. Furthermore, the structural effects which have been observed must have an influence on glass formation, although this aspect of the problem has not yet been adequately studied.

Table XXIV

$$B_p = d[a_3 n + b_3]^{c_3}$$

$$a_3 = 8.1227 \times 10^6$$

$$b_3 = 3.7871 \times 10^7$$

$$c_3 = 4.1048 \times 10^{-1}$$

<u>n</u>	<u>Calculated B_p</u>	<u>(Observed B - Calculated B)_p</u>
3	779.74	33.46
4	953.52	-7.62
5	1081.44	-16.81
6	1186.632	-15.102
7	1277.565	-9.450
8	1358.330	-3.204
9	1432.113	-3.302
10	1499.958	1.310
11	1562.925	9.552
12	1621.945	3.983
13	1678.023	11.070
14	1731.141	8.482
15	1781.934	7.724
16	1830.668	0.649
17	1877.27	3.34
18	1922.30	-1.70
19	1965.7	-4.1
20	2007.5	-13.5

Table XXV

$$T_{o_p} = B_p (a_4 n + b_4)^{c_4}$$

$$a_4 = 7.6210 \times 10^{-5}$$

$$b_4 = 3.7362 \times 10^{-5}$$

$$c_4 = 4.07977 \times 10^{-1}$$

<u>n</u>	<u>Calculated T_o</u>	<u>(Observed T_o - Calculated T_o)</u>
3	24.73	0.43
4	32.98	0.18
5	41.12	0.04
6	49.099	-0.305
7	56.889	-0.629
8	64.442	-0.799
9	71.501	0.040
10	78.611	0.069
11	85.768	-0.630
12	92.033	0.816
13	98.914	-0.037
14	105.120	0.506
15	111.341	0.528
16	117.073	1.559
17	123.328	-0.188
18	129.01	-0.38
19	134.78	-1.22
20	139.98	-0.02

Table XXVI

$$T_o = \frac{d}{m} [a_5 n + b_5]^{c_5}$$

$$a_5 = 2.3518 \times 10$$

$$b_5 = 7.8325$$

$$c_5 = 1.7555$$

<u>n</u>	<u>Calculated T_o</u>	<u>(Observed T_o - Calculated T_o)</u>
3	23.64	1.52
4	33.05	0.11
5	41.58	-0.42
6	49.598	-0.804
7	57.257	-0.997
8	64.619	-0.976
9	71.760	-0.219
10	78.689	-0.009
11	85.430	-0.292
12	92.007	0.842
13	98.461	0.416
14	104.779	0.847
15	110.989	0.880
16	117.099	1.533
17	123.098	0.042
18	129.014	-0.384
19	134.844	-1.284
20	140.583	-0.623

Table XXVII

$$T_o = d[a_6 n + b_6]^{c_6}$$

$$a_6 = 4.6879 \times 10$$

$$b_6 = 2.7514 \times 10$$

$$c_6 = 7.5484 \times 10^{-1}$$

<u>n</u>	<u>Calculated T_o</u>	<u>(Observed T_o - Calculated T_o)</u>
3	23.59	1.57
4	33.03	0.13
5	41.56	-0.40
6	49.596	-0.802
7	57.262	-1.002
8	64.627	-0.984
9	71.771	-0.230
10	78.702	-0.022
11	85.442	-0.304
12	92.018	0.831
13	98.471	0.406
14	104.787	0.839
15	110.994	0.875
16	117.100	1.532
17	123.095	0.045
18	129.01	-0.38
19	134.83	-1.27
20	140.57	-0.61

TABLE XXVIII
Correlation for Intermolecular Interactions

Compound	Bp	V	Q	n	s	$Q - n + 0.15s - 0.876$
2-Methylpropane	882.80	105.48	4.738	4	1	0.012
2-Methylbutane	1020.012	117.383	5.684	5	1	-0.042
2-Methylpentane	1135.410	132.875	6.719	6	1	-0.007
2-Methylhexane	1236.026	148.576	7.747	7	1	0.021
2-Methylheptane	1337.468	164.607	8.834	8	1	0.108
2-Methyloctane	1410.0	180.74	9.821	9	1	0.095
3-Methylpentane	1152.368	130.611	6.707	6	1	-0.019
3-Methylhexane	1240.196	146.714	7.695	7	1	-0.031
3-Methylheptane	1331.530	162.770	8.734	8	1	0.008
3-Methyloctane	1411.0	178.92	9.754	9	1	0.028
2,2-Dimethylpropane	950.84	123.31	5.598	5	2	0.028
2,2-Dimethylbutane	1081.176	133.712	6.515	6	2	-0.061
2,2-Dimethylpentane	1190.033	149.654	7.576	7	2	0
2,2-Dimethylhexane	1273.594	165.274	8.551	8	2	-0.025
2,2-Dimethylheptane	1355.0	181.50	9.571	9	2	-0.005
2,4-Dimethylpentane	1192.041	149.925	7.596	7	2	0.020
2,4-Dimethylhexane	1287.876	164.068	8.575	8	2	-0.001
2,4-Dimethylheptane	1360	180.25	9.548	9	2	-0.028

Table XXIX

Effect of Vicinal Side Groups on Q

	B_p	V	Q	n	s	v	$Q-n + 0.15s$ $-0.035v - 0.876$
2,3-Dimethylbutane	1127.187	131.156	6.621	6	2	1	0.010
2,3-Dimethylpentane	1238.017	145.023	7.621	7	2	1	0.010
2,3-Dimethylhexane	1315.503	161.313	8.602	8	2	1	-0.009
2,3-Dimethylheptane	1392	177.61	9.608	9	2	1	-0.003
2,2,4,4-Tetramethylpentane	1325.183	179.213	9.332	9	4	0	0.056
2,3,3,4-Tetramethylpentane	1417.473	170.743	9.461	9	4	4	0.045
2,2,5-Trimethylhexane	1324.049	182.375	9.445	9	3	0	0.019
3,3,4-Trimethylhexane	1401.0	172.98	9.470	9	3	2	-0.026
3-Methyl-4-ethylhexane	1399	173.8	9.492	9	2	1	-0.119
2-Methyl-4-ethylhexane	1362	178.4	9.488	9	2	0	-0.088
4-Ethylheptane	1397	176.7	9.597	9	1	0	-0.129
3-Ethylhexane	1327.884	160.997	8.648	8	1	0	-0.078
2,4-Dimethyl-3-ethylpentane	1389.0	174.70	9.479	9	3	2	-0.017
2,3-Dimethyl-3-ethylpentane	1414	171.0	9.454	9	3	2	-0.042
3,3-Diethylpentane	1451.245	171.000	9.634	9	2	0	0.058
3-Methyl-3-ethylhexane	1404	174.0	9.525	9	2	0	-0.051
3-Methyl-3-ethylpentane	1347.209	157.868	8.616	8	2	0	0.040
2-Methyl-3-ethylpentane	1318.120	159.704	8.552	8	2	1	-0.059
3-Ethylpentane	1251.827	144.388	7.658	7	1	0	-0.068
4-Propylheptane	1515	194.21	10.897	10	1	0	0.171
4-Isopropylheptane	1508	193.0	10.814	10	2	1	0.203
2,2,3,3-Tetramethylpentane	1397.483	170.32	9.347	9	4	4	-0.069
3-Isopropyl-2-methylhexane	1519	190.5	10.766	10	3	2	0.270
3,4-Diethylhexane	1515	189.7	10.714	10	2	1	0.103
2,3,4,5-Tetramethylhexane	1474.1	188.9	10.474	10	4	3	0.093
3-Isopropyl-2,4-dimethylpentane	1468.4	188.552	10.428	10	4	3	0.047
2,2,3,3,4-Pentamethylpentane	1496.1	183.168	10.351	10	5	6	0.015

References

1. A. A. Miller, J. Polymer Sci., 1, 1857 (1963).
2. G. S. Fulcher, J. Am. Ceram. Soc., 8, 339 (1925).
3. G. Tammann and W. Hesse, Z. Anorg. Chem., 156, 245 (1926).
4. J. D. Ferry, Viscoelastic Properties of Polymers, (John Wiley & Sons, Inc., New York, 1961).
5. J. H. Gibbs, J. Chem. Phys., 25, 185 (1956); J. H. Gibbs and E. A. DiMarzio, ibid., 28, 373 (1958); ibid., 28, 807 (1958); J. Polymer Sci., 1, 1417 (1963).
6. W. Kauzman, Chem. Revs., 43, 219 (1948).
7. "Selected Values of Properties of Hydrocarbons and Related Compounds," American Petroleum Institute Research Project 44, Carnegie Institute of Technology, Vol. II, Tables 20C (part 1) and 20C-K (part 1), 1952.
8. A. K. Doolittle, J. Appl. Phys., 22, 1032 (1951).
9. S. Glasstone, K. J. Laidler and H. Eyring, The Theory of Rate Processes, (McGraw-Hill Book Company, Inc., New York and London, 1941).
10. L. R. G. Treloar, The Physics of Rubber Elasticity, (Oxford University Press, Amen House, London E.C.4).
11. L. H. Tung, J. Polymer Sci., 46, 409 (1960).
12. S. L. Aggarwal, L. Marker and M. J. Corrano, J. Appl. Polymer Sci., 3, 77 (1960).
13. L. Marker, R. Early and S. L. Aggarwal, J. Polymer Sci., 38, 381 (1959).
14. M. K. Karapetyants & K. S. Yan, Izv. Vyassaikh Uchebn. Zavedenii, 4, 580 (1961); Ca 56, 13567 b.
15. T. G. Fox and P. J. Flory, J. Appl. Phys., 21, 581 (1950).
16. M. L. Williams, J. Appl. Phys., 29, 1395 (1958).
17. D. A. Lowitz, J. W. Spencer, W. Webb & R. W. Schiessler, J. Chem. Phys., 30, 73 (1959).

18. J. M. O'Reilly, J. Polymer Sci., 57, 429 (1962).
19. W. G. Cutler, R. H. McMickle, W. Webb, and R. W. Schiessler, J. Chem. Phys., 29, 727 (1958).
20. J. D. Ferry, "Viscoelastic Properties of Polymers", p. 228, John Wiley and Sons, Inc., N. Y., 1961.
21. U. Bianchi, J. Polymer Sci., A2, 3083 (1964).
22. A. Ciferri, J. Polymer Sci., A2, 3089 (1964).
23. O. B. Ptitsyn, Vysokomol. Soed., 5, 1219 (1963); Polymer Science USSR 5, 289 (1964).
24. D. J. Millen, Progress in Stereochemistry (Butterworth, Inc., Washington, D.C., 1962) p. 160.
25. M. L. Huggins, Ann. N. Y. Acad. Sci., 41, 1 (1942).
26. P. J. Flory, J. Chem. Phys., 10, 51 (1942).
27. P. J. Flory, Proc. Royal Soc. (London), A234, 60 (1956).
28. S. Lifson, J. Chem. Phys., 30, 964 (1959).
29. K. Nagai and T. Ishikawa, J. Chem. Phys., 37, 496 (1962).
30. C. A. Hoeve, J. Chem. Phys., 35, 1266 (1961).
31. H. W. Starkweather, Jr. and R. H. Boyd, J. Phys. Chem., 64, 410 (1960).
32. W. J. Taylor, J. Chem. Phys., 1b, 257 (1948).
33. M. H. Cohen and D. Turnbull, J. Chem. Phys., 31, 1164 (1959).
34. M. M. Kreevoy and E. A. Mason, J. Am. Chem. Soc., 79, 4851 (1957).
35. P. DeSantis, E. Giglio, A. M. Liquori and A. Ripamonti, J. Polymer Sci., A1, 1383 (1963).
36. T. A. Orofino and A. Ciferri, J. Phys. Chem., 68, 3k36 (1964).
37. K. S. Pitzer, J. Chem. Phys., 8, 711 (1940).
38. R. P. Smith, J. Chem. Phys., 42, 1162 (1965).
39. J. W. L. Fordham, J. Polymer Sci., 39, 321 (1959).

40. S. Mizushima and T. Shimanouchi, J. Am. Chem. Soc., 86, 3521 (1964).
41. I. Sakurada, A. Nakajima, O. Yoshizaki and K. Nakamae, Kolloid Z., 186, 41 (1962).
42. A. J. Barlow, G. Harrison and J. Lamb, Proc. Roy. Soc., A282, 228 (1964).
43. S. Saito, Kolloid Z., 189, 116 (1963); also "Study of Molecular Motions in Solid Polymers by the Dielectric Measurements", No. 648, Researches of the Electrotechnical Laboratory, Agency of Industrial Science and Technology, Japan, 1964.
44. T. L. Hill "Statistical Mechanics", McGraw-Hill, New York, 1956. Ch. 8.
45. J. Hirschfelder, D. Stevenson, and H. Eyring, J. Chem. Phys., 5, 896 (1937),
46. O. K. Rice, J. Chem. Phys. 6, 476 (1938).
47. R. W. Gurney and N. F. Mott, J. Chem. Phys., 6, 222 (1938).
48. F. Bueche, "Physical Properties of Polymers", Interscience, New York, 1962.
49. M. Kurata and W. H. Stockmayer, Fortschr. Hochpolymeren Forsch., 3, 196 (1963).
50. T. G. Fox and P. J. Flory, J. Polymer Sci., 14, 315 (1954).
51. T. G. Fox and P. J. Flory, J. Phys. Chem., 55, 221 (1951).
52. P. J. Flory, J. Am. Chem. Soc., 62, 1057 (1940).
53. J. D. Ferry and G. S. Parks, J. Chem. Phys., 4, 70 (1936).
54. B. M. Grieverson, Polymer, 1, 499 (1960).
55. R. Nakatsuka, Bull. Chem. Soc., Japan, 37, 403 (1964).
56. T. G. Fox and S. Loshaek, J. Polymer Sci., 15, 371 (1955).
57. A. A. Miller, J. Phys. Chem., 67, 1031 (1963).
58. C. A. Angell, J. Phys. Chem., 68, 218 (1964); 68, 1917 (1964).
59. F. Gutmann and L. M. Simmons, J. Appl. Phys., 23, 977 (1952).

- 60. D. W. Davidson and R. H. Cole, J. Chem. Phys., 19, 1484 (1951).
- 61. W. Kauzmann, Revs. Mod. Phys., 14, 12 (1942).
- 62. See, for example, A. J. Curtis in "Progress in Dielectrics", Vol. 2, J. B. Birks, ed., John Wiley, New York, 1960.
- 63. W. Sommer, Kolloid Z., 167, 97 (1959).
- 64. S. Saito and T. Nakajima, J. Appl. Polymer Sci., 2, 93 (1959).
- 65. P. A. Small, J. Appl. Chem., 3, 71 (1953).
- 66. R. R. Dreisbach, "Physical Properties of Chemical Compounds II", American Chemical Society, Washington, D. C., 1959.

UNCLASSIFIED

Security Classification

DOCUMENT CONTROL DATA - R&D

(Security classification of title, body of abstract and indexing annotation must be entered when the overall report is classified)

1. ORIGINATING ACTIVITY (Corporate author) American Cyanamid Company 1937 West Main Street Stamford, Connecticut 06904		2a. REPORT SECURITY CLASSIFICATION Unclassified	
		2b. GROUP - -	
3. REPORT TITLE The Relationships between Polymers and Glass Transition Temperatures			
4. DESCRIPTIVE NOTES (Type of report and inclusive dates) Final Summary Report (June 1963 - May 1965)			
5. AUTHOR(S) (Last name, first name, initial) Lewis, O. G. and Gallacher, L. V.			
6. REPORT DATE July 1965		7a. TOTAL NO. OF PAGES 74	7b. NO. OF REFS 59
8a. CONTRACT OR GRANT NO. AF 33(657)-11224 b. PROJECT NO. 7342 c. Task No. 734203 d.		9a. ORIGINATOR'S REPORT NUMBER(S) AFML-TR-65-231 9b. OTHER REPORT NO(S) (Any other numbers that may be assigned this report) - -	
10. AVAILABILITY/LIMITATION NOTICES Qualified requesters may obtain copies of this report from the Defense Documentation Center. This report has been released to CFSTI for sale to the general public.			
11. SUPPLEMENTARY NOTES - - -		12. SPONSORING MILITARY ACTIVITY Nonmetallic Materials Division, Air Force Materials Laboratory, Research & Technology Div., Air Force Systems Command, WPAFB, O.	
13. ABSTRACT A study of some empirical and theoretical functions for the effect of temperature on liquid viscosity indicated that the viscosities of the n-alkanes are well represented by the equation $\log (\eta/d) = \log (A/T) + B/(T-T_0)$, where d is the density and A, B and T_0 are smooth functions of chain length. A relaxation theory developed by J.H. Gibbs relates B to the barrier to rotation about chain bonds. The T_0 (n) values are predicted for n-alkanes of more than n=6 carbon atoms by the Gibbs-DiMarzio theory with a flex energy of 490.8 cal./mole, in agreement with estimates by other methods. An empirical approach to estimation of flex energy and hence T_0 is suggested. A statistical-mechanical theory of the glass transition was developed, based on the concept that the observable communal entropy is time dependent. Glass temperatures are theoretically predicted with good accuracy from viscosity data obtained far above T_g . The activation free energy, enthalpy and entropy at the glass temperature were evaluated for several polymers. Intermolecular interactions in liquid alkanes were studied, and an additive property $Q=(B_p V)^{0.7240}$ was found, where B_p is the Antoine vapor pressure constant, and V the molar volume.			

DD FORM 1473
1 JAN 64Unclassified
Security Classification